Master of Science Thesis

Estimation of neutron dose contributions to personnel working around high-energy medical linear accelerators for radiation therapy.

Drita Muca

Supervisors: Charlotte Thornberg,
Sören Mattsson and Anja Almén

This work has been performed at the Department of Medical Radiation Physics, Malmö University Hospital/Lund University.

Medical Radiation Physics
Clinical Sciences, Lund
Lund University, 2006

Contents

Abstract

Purpose: Medical linear accelerators that operate above 10 MeV produce neutrons by photonuclear reactions which present a potential radiation hazard to the personnel. The purpose of this study was to estimate neutron dose contributions to the personnel working with external radiotherapy at Malmö University Hospital (UMAS), compare different kind of neutron detectors/dosemeters, and evaluate how to translate the results of the measurements to an effective dose. By estimating the neutron doses received by the personnel one can decide if better shielding is required.

Method: Two accelerators that operate above 10 MeV, Varian Clinac 2100 C/D and Elekta precise, were investigated. Measurements with area monitoring devices (BF_3 and ^3He based instruments) were performed outside the treatment room (in experimental form), to make a survey of the neutron dose equivalent rate around the radiotherapy facility. Measurements were also performed inside the control rooms when the accelerators were in clinical use (during patient treatment). The personnel were carrying different kind of personal neutron dosemeters (electronic dosemeters, bubble detectors and etched-track detectors) during their time of work. The relation between the operational quantities and the protection quantities were studied.

Results and Discussion: It was found that the highest neutron dose rates outside the treatment room when irradiating a phantom with 18 MV photon beams from the Elekta machine, were outside the treatment door (~150 μSv/h), at the hallway between the control rooms (~90 μSv/h), and inside one of the control rooms (~40 μSv/h). Furthermore from this machine, the neutron contribution to the measured dose equivalent rate was higher than the photon component. The estimated neutron dose equivalent varied up to a factor of two and occasionally even more for the different measuring devices. The highest personal dose equivalent from the personal dosemeters was estimated to be in the order of about 1 mSv/year. The personal dose equivalent is the most appropriate operational quantity for estimating the effective dose while the ambient dose equivalent is a rough approximation of the effective dose.

Conclusions: This study shows that the neutron component from the bunker with the Elekta machine needs to be considered when high-energy photon beams are used. The measure that could be taken in order to reduce the neutron dose to the personnel is to avoid 18 MV treatments in that bunker. Another solution is to build an additional "neutron stopping door" with hydrogen-containing shielding material inside the treatment room that has to be closed during 18 MV treatments.

Populärvetenskaplig sammanfattning

Strålning kan medföra både skada och nytta. Inom strålbehandling utnyttjas strålningen för att bota eller lindra cancersjukdomar. Målet är att med hjälp av joniserande strålning slå ut alla tumörceller samtidigt som man försöker skona övriga friska celler. Strålningen som produceras i den vanligaste utrustningen för extern strålbehandling, nämligen linjäraccelerator, är elektronstrålning och fotonstrålning av varierande energi. Strålslag och energi bestäms beroende på hur djupt in i kroppen man vill att strålningen ska tränga in.

För att kunna behandla en djupt liggande tumör används normalt högenergetisk fotonstrålning. Vid dessa höga fotonenergier genereras oönskade neutroner och produktionen ökar med fotonenergin. Neutronerna stannar inte bara i behandlingsrummet utan kan gå igenom väggar och dörrar, som i första hand är avsedda som strålskydd för fotoner och elektroner. Neutroner ger därmed stråldos till personal.

Strålmiljön runt linjäracceleratorerna berör personal som arbetar med behandlingarna. För att kontrollera stråldosen till personal bär de en så kallad dosimeter som mäter hur stor stråldos användaren har utsatts för. Dessa dosimetrar mäter normalt bara fotondosbidraget och inte dosbidraget från neutroner.

Målet med detta arbete var att kartlägga neutrondosbidraget till personalen som arbetar med strålbehandling i Universitetssjukhuset MAS i Malmö. Olika typer av neutron-mätinstrument användes och jämfördes. Mätningar gjorde dels i form av experimentella mätningar och dels när acceleratorn var i klinisk drift vid patientbehandlingar.

Resultaten visade högre bidrag till stråldosen från neutroner än från fotoner från en av bunkrarna vid behandling med högsta fotonenergin. Neutronbidraget får inte försummas och de åtgärder som kan göras är antingen att inte göra behandlingar med högsta fotonenergin på den acceleratorn eller om detta inte är praktiskt möjligt, bygga en extra ”neutron dörr” inne i behandlingsrummet.

1. Introduction

Linear accelerators (linacs) for cancer radiotherapy accelerate electrons that produce high-energy bremsstrahlung photon beams (i.e. x-rays). Accelerators operating above about 10 MeV produce fast neutrons whose angular distribution is almost isotropic. Below 10 MeV neutron production is negligible [1]. Neutrons from medical linacs are mainly produced through photonuclear (γ,n) reactions and the production increases with photon energy. These photoneutrons contaminate the therapeutic beam and are of concern to the personnel working around the treatment room.

Personnel doses from gamma- and x-rays have been studied in several earlier [2, 3]. The personnel normally wear thermoluminescent dosemeters (TLD) for estimation of the dose equivalent from photons. Since neutron interaction is complicated, neutron doses are difficult to measure. The purpose of this study was to investigate and evaluate methods of estimating neutron dose contributions to the personnel working with external radiotherapy at Malmö University Hospital (UMAS). Different kinds of neutron detectors were used and measurements were made outside the treatment room both in experimental form and when the accelerators were in clinical use (during patient treatment). The personnel were also carrying different kind of additional personal dosemeters during their work. By estimating the neutron doses received by the personnel, one can decide if better shielding requirements are necessary.

The neutron environment outside the treatment room will depend on several factors such as the design of the accelerator, the room shielding, geometric circumstances, the gantry angle, and the materials in the path of the photon beam. Furthermore, the neutron doses received by the personnel will depend on were they are staying and for how long. Since high-energy photons are usually used for deep-seated tumours rather than high-energy electrons, and since the cross section for electronuclear reactions is small, focus will lie on neutron production by high-energy photons.

2. Background

2.1 Neutron production

A nucleus can absorb energy from a high-energy photon or a high-energy electron and emit a neutron if the energy of the photon or electron exceeds the minimum energy that requires to remove a neutron from a nucleus. This separation energy decreases with the increase of the target atomic number [4] and lies, for most stable nuclei heavier than carbon, between 6 and 16 MeV [1]. The cross section for neutron production increases as the photon energy, above the separation energy required to emit a neutron from a nucleus, increases but will decrease with further increasing of photon energy after reaching a maximum value. This is characteristic of resonance reactions and is called the *giant resonance*. Depending on if the target nucleus is a light or heavy element, the giant resonance region lies in the photon energy interval between 13-25 MeV where the cross section is maximum and has a sharply peaked structure [1, 5]. The cross section of the various types of neutron interactions in most materials is a strong function of neutron energy and is usually highest at low neutron energies. A typical neutron cross-section curve shows many distinct resonances or cross-section peaks that normally occur at higher neutron energies. These resonances arise when the neutron energy correspond to an energy level in the atomic nucleus where the nucleus is very sensitive for reaction [6]. A good illustration for this is figure 1.

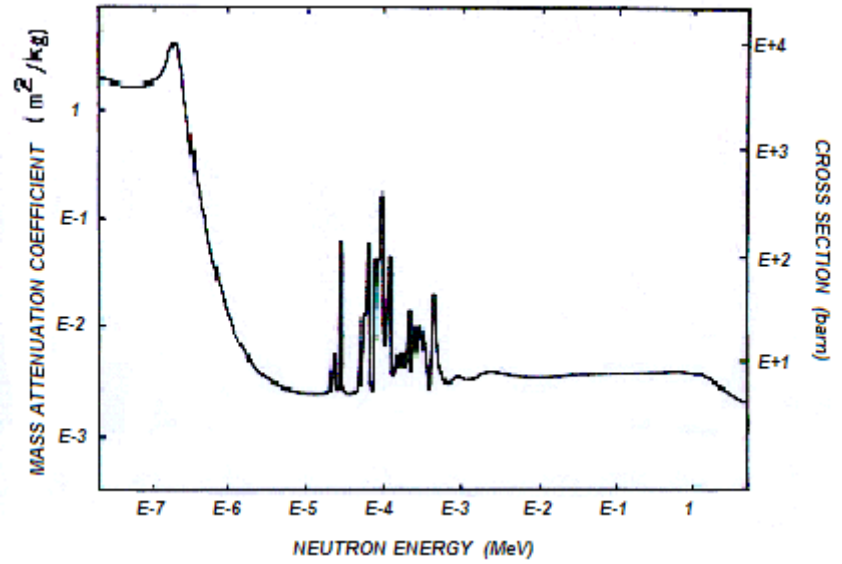

Figure 1. The total neutron cross section and mass attenuation coefficient for cadmium as a function of incident neutron energy [7].

The contribution from neutron production through electronuclear reactions in medical linear accelerators is usually negligible because high-energy photons are usually used for deep-seated tumours rather than high-energy electrons and because the cross section for these reactions inside the treatment head is small. The cross section for electronuclear reactions is about 137 times smaller than photonuclear reactions [8]. Neutrons can also be produced by other photodisintegration processes like (γ, 2n) and (γ, pn) or through photon- or electron-induced fission. Nuclei heavier than bismuth undergo fission when bombarded with electrons or photons. This fission process is less important because it is usually negligible below about

5 MeV [1]. Since the (γ, 2n) and (γ, pn) reactions have smaller cross sections [8], photonuclear reactions (γ, n) are the main cause of neutron contamination in external radiotherapy.

Inside the linac treatment room there is a mixed radiation field of the treatment photons (or electrons) and the produced neutrons. The sources of the undesired photoneutrons are in summary any materials on which the photon beam is incident. The most important neutron sources are materials inside the linac head like the target, flattening filters and collimating devices where the photon fluence and the target atomic number is high [1, 4, 8]. The neutron production also depends to a large extent on the materials' isotopic composition. The treatment room walls, the floor and the path of the photon beam including air and the patient's body are other photoneutron sources that will add less to the neutron component [4]. The neutrons further scattering or absorption will depend on what energy they have and which materials they hit.

Neutrons that pass through the walls and doors of the treatment room have a spectra of different energies and are of concern for the operating personnel. In general, neutron angular distribution is isotropic and the average energy of the neutron spectrum obtained by photonuclear reactions is around a few MeV [4, 8]. The photoneutron spectrum is quite similar to the ^{252}Cf fission neutron spectrum and many neutron detectors are calibrated against this neutron source. After penetration of the accelerator head, which is usually in a concrete-shielded room, the photoneutron spectrum changes to a degraded fission spectrum since room-scattered neutrons will further soften the spectrum [1]. Outside the room of the linear accelerator, the average neutron energy is lower (less than about 0.5 MeV) than inside the treatment room.

2.2 Neutron interactions

Since neutrons have no electric charge they can't interact through electrical processes but only through nuclear reactions, unlike the photons where interactions with the atomic electrons also is significant. The cross section for interaction (per atom) depends on the energy of the neutron and varies strongly with the composition of the absorbing material. When a neutron undergo interaction it may either totally disappear and be replaced by one or more secondary radiations, or else the energy or direction of the neutron is changed significantly. Neutron reactions can be divided in elastic scattering and absorption reactions where the latter can be further subdivided into particle emission, radiative capture and inelastic scattering. The probability of the various types of reactions varies with the neutron energy. The possible neutron kinetic energies, E_n, can be classified as [7]

1. Slow neutrons: $0 \leq E_n < 1$ keV
2. Intermediate neutrons: 1 keV $\leq E_n <$ 0.5 MeV
3. Fast neutrons: $E_n \geq 0.5$ MeV

Among the slow neutron category are the well-known thermal neutrons that are in thermal equilibrium with their surroundings and at room temperature of 20°C have a maximum energy at 0.025 eV [7]. At this level the neutron kinetic energy is similar to the average kinetic energy of the molecules in a room temperature gas and occures after a large number of collisions with nuclear targets. Thermal neutrons have a much larger effective cross-section than fast neutrons and can therefore be absorbed more easily by any atomic nuclei that they collide with, creating a heavier - and often unstable – isotope as a result.

2.2.1 Elastic scattering

Elastic neutron scattering (n,n) is an important interaction for the detection of fast and intermediate neutrons in most light nuclei, and often tend to bring the neutrons into thermal equilibrium with the absorber material. In elastic scattering, an incoming neutron interacts with a target nucleus and then gets a different direction and a reduction in kinetic energy. The energy loss of the neutron is transferred to the recoiling nucleus, which moves away at an increased speed, which is given by equation (1) [9, 10]:

$$E_{tr} = E_n \frac{4A}{(1+A)^2} \cos^2 \theta \,, \tag{1}$$

where E_{tr} is the transferred energy and thus the kinetic energy of the recoiling nucleus, A is the mass of target nucleus, E_n is the incident neutron energy, and θ is the scattering angle of the recoil nucleus in the laboratory system (see figure 2).

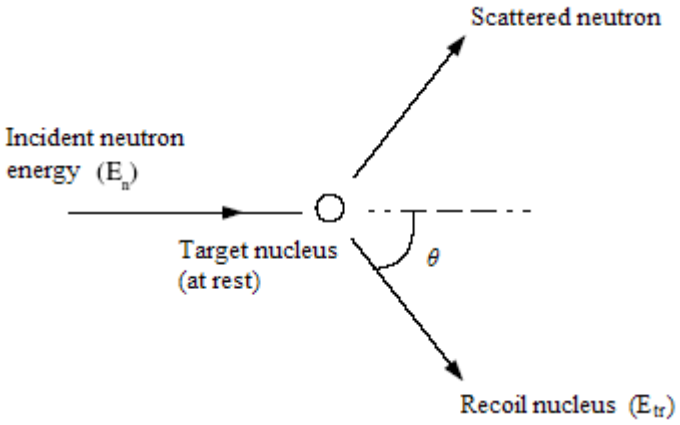

Figure 2. Schematic chart of elastic scattering in the laboratory system.

The Q-value for elastic scattering is zero because the total kinetic energy is conserved (the energy after the reaction is the same as before the reaction) [9]. The Q-value is the minium energy necessary to induce a reaction and since the target nucleus is at rest in the laboratory system, the sum of the kinetic energies of the reaction products is the same as the incoming neutron energy. As can be seen from equation (1) the transferred energy to the recoiling nucleus becomes larger with increasing neutron energy. Thus slow neutrons, with small kinetic energies, can only transfer very little energy to the nucleus in elastic scattering. For higher neutron energies the transferred energy becomes greater and after a number of collisions the neutrons are slowed down to lower energies. The transferred energy also depends on the scattering angle so that the recoil energy is maximum when $\theta \cong 0$, i.e. when the recoil nucleus is emitted in the same direction as the incoming neutron [9]. The maximum energy transfer is given by equation (2) [9]:

$$E_{tr}(\max) = E_n \frac{4A}{(1+A)^2} \tag{2}$$

The maximum possible neutron energy transfer to the recoil nucleus in a single collision is the total neutron kinetic energy and is greatest when the mass of the nucleus is the smallest [7, 9]. This occurs with hydrogen, because here the neutron and the hydrogen nucleus (one proton) have about the same mass. For heavier elements the maximum energy transfer is always less. Therefore hydrogen is often used in neutron shielding materials where the neutron can lose up to all of its energy in one single collision with the hydrogen nucleus. The interaction with hydrogen is also important because of the large amounts of hydrogen in tissue and gives the greatest contribution to the absorbed dose from neutron exposure [6].

2.2.2 Absorption reactions

In an absorption reaction the incident neutron disappears inside the nucleus and secondary radiations are emitted after the process which can be directly detected. The secondary radiations resulting from neutron interactions may be heavy charged particles, photons from *radiative capture* reactions (n,γ), or another neutron from *inelastic scattering* (n,n').

The radiative capture reaction is the dominant absorption reaction in most medium and heavy nuclear targets, for slow and intermediate neutrons [7]. In general the reaction is exoergic (i.e. $Q > 0$) to make it energetically possible, because the incident neutron energy is so low. The value of the radiative capture thermal neutron cross-section and the energy of the emitted gamma ray are interesting for shielding purposes and vary with the target nucleus. For most neutron detectors the gamma rays from radiative capture reactions are difficult to detect. Instead *particle emission* reactions are more desirable where the secondary radiations are charged particles that are easier to detect. Particle emission reactions are important in the fast neutron region but may also dominate in the slow and intermediate energy region if the reaction is exoergic [7]. The secondary particles from these reactions might be protons, deuterons, alpha particles, recoil nuclei or fission products. In some cases the residual nucleus may be left in an excited state and emission of gamma rays then follows.

The inelastic scattering (n,n') is an important process in the fast neutron region where a neutron may be momentarily absorbed in a nucleus and then emitted with reduced energy [9]. After the scattering the nucleus is left in an excited state, which quickly de-excites by gamma emission. The threshold for this reaction varies widely with the target nucleus and depends on the energy of the first excited state. For light nuclei this threshold energy may be quite high, being 6.44 MeV in ^{16}O and 4.80 MeV in ^{12}C [7]. Inelastic scattering plays an important role in the shielding of high-energy neutrons.

2.3 Quantities used in radiological protection

In radiological protection two types of quantities are of importance: *protection quantities*, which are defined by the ICRP, and *operational quantities*, which are defined by the ICRU. In order to estimate the effective dose to the personnel, the measured values (i.e. the operational quantities) need to be translated into relevant protection quantities, and the performance of the operational quantities need to be studied.

The protection and operational quantities can be related to basic physical quantities: particle fluence (Φ), air kerma free-in-air (K_a), and the tissue-absorbed dose (D). This is done with recommended conversion coefficients, which has been recently updated for neutrons. The

conversion coefficients are calculated from various mathematical models and measurement phantoms.

The relationship of the quantities used in radiological protection is illustrated in figure 3. ICRU 1998 [11] and ICRP 1996 [12] give the conversion coefficients between different quantities.

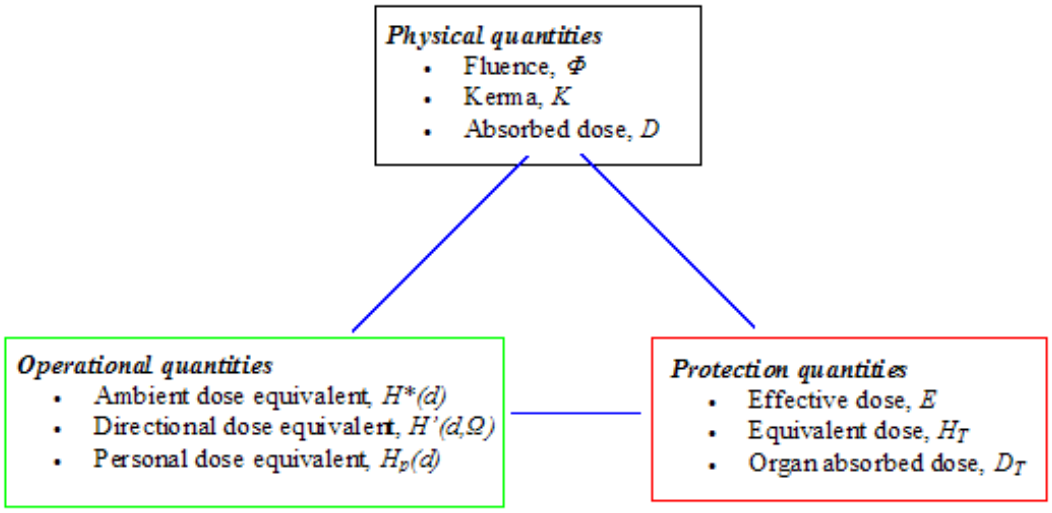

Figure 3. The quantities used in radiological protection.

2.3.1 Protection quantities

The most important protection quantity in radiation protection according to ICRP 1990 [13] is the effective dose, E. This quantity is a total body dose and can not be measured directly. Other important protection quantities for use in radiological protection are the mean absorbed dose in an organ or tissue, D_T, and the equivalent dose in an organ or tissue, H_T. These quantities are defined in appendix I. The protection quantities are not directly measurable but may be calculated if the conditions of irradiation are known.

2.3.2 Operational quantities

The operational quantities are related to the protection quantities and intended to provide an appropriate estimate of the protection quantities. They are measurable and intended for external radiation. The operational quantities applicable for whole-body irradiations with neutrons are [14]: the ambient dose equivalent, $H^*(10)$, for area monitoring and the personal dose equivalent, $H_p(10)$, for individual monitoring, which are defined in appendix I. These quantities have different relations to the effective dose and may result in that personal dosemeters and instruments for area monitoring show different numerical values in the same irradiation situation. The differences vary and are caused by the geometry of the radiation field. Personal dosemeters which are worn on the body may be influenced by the body's backscatter and the personal dose equivalent can vary both between individuals and between locations on any given individual.

The operational quantities were designed to avoid underestimation or excessive overestimation of the appropriate protection quantity, so that the value of the operational

quantity should be higher than that of the protection quantity. For example, in the absence of the value of the effective dose you only have the value of the ambient dose equivalent, then the effective dose is to be overestimated and presumably no need to be determined. During the last few years changes in both ICRP and ICRU recommendations have affected the operational quantities. Therefore it is important to verify if the operational quantities continue to present a suitable measurement of the protection quantities.

In the description of the operational quantities, ICRU has defined a phantom replacing the body. This tissue-like phantom is called the *ICRU sphere* (30 cm diameter) and has a mass composition of 76.2% oxygen, 11.1% carbon, 10.1% hydrogen and 2.6% nitrogen [14, 15]. For the purpose of dosemeter calibration and other practical activity, ICRU recommends that the sphere is replaced with a slab phantom (cuboid: 30cm×30cm×15cm) of the same mass composition [14, 15].

2.3.3 Relations between the operational quantities and the protection quantities

The relations between the operational and protection quantities can be calculated using conversion coefficients, and depend on the irradiation geometry. In general, neutrons incident perpendicular on the front of the body generate the largest effective dose since most radiation sensitive organs are situated closer to the front of the body than to the back [12]. The different irradiation geometries are [12, 15]:

- **AP** geometry; radiation incident perpendicular on the front of the body.
- **PA** geometry; radiation incident perpendicular from behind of the body.
- **LAT** geometry; irradiation from the side perpendicular to the body. **LLAT** means irradiation from the left, and **RLAT** irradiation from the right.
- **ROT** geometry; irradiation in a 360º rotating plane parallel beam.
- **ISO** geometry; irradiation in a fully isotropic radiation field.

The first three geometries are best described in situations where a person has its body all the time in some of these geometries. If the person walks around the radiation field in a random way the situation is better described with the rotation geometry. The isotropic geometry can be related to situations were the radiation source is a radioactive gas that surrounds the person.

The relation between the effective dose and the operational quantities is examined in the ICRP 1996 [12] and the ICRU 1998 [11]. A general relation between effective dose and personal dose equivalent is difficult to give since the personal dose equivalent is dependent on whom and how the personal dosemeter is worn. Figure 4 shows the relationship between the effective dose and the ambient dose equivalent as a function of neutron energy for all the different irradiation geometries. Except for the AP and PA geometry the ambient dose equivalent overestimates the effective dose up to incident neutron energies of 40 MeV. In some energy regions the ambient dose equivalent underestimates the effective dose, particularly in the AP geometry from about 1 eV to 40 keV but also in the higher energy regions in all geometries.

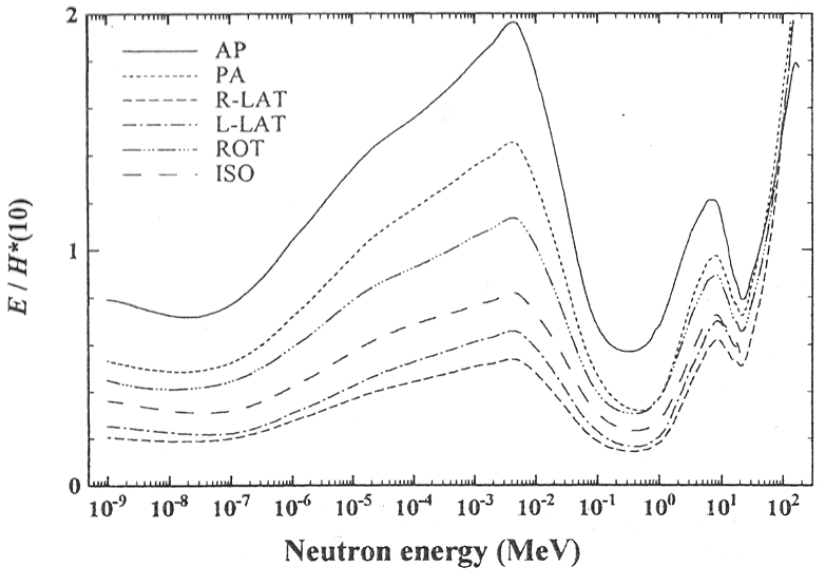

Figure 4. The ratio of *E/H*(10)* as a function of neutron energy for different irradiation geometries [12].

In practice monoenergetic radiation fields are rare and the energies of the neutrons extend over a wide range. Several studies at facilities in the nuclear industry have been performed for a variety of neutron spectra [12]. These studies indicate that the typical neutron spectra show peaks in the energy range between 100 keV and 1 MeV, which is characteristic of degraded fission neutrons. In this energy region the ratio *E/H*(10)* show that in all irradiation geometries the ambient dose equivalent presents a reasonable overestimate of the effective dose.

Another study at Ringhals nuclear power plant in Sweden was also performed for a variety of neutron spectra which have been measured in some positions of interest L, A, F and G within the containment of a pressurized water reactor (see figure 5) [15]. D, E and P are points of measuring close to a transport container filled with spent nuclear fuel placed at Clab, a central storage facility in Sweden. The personal dose equivalent could be calculated since the neutron fluence and the direction distribution of the fluence had been determined in experimental way. The ratio $H_p(10)/E$ in figure 5 shows that the personal dose equivalent provides a good estimate of the effective dose in these neutron fields. The ratio *H*(10)/E* shows that the ambient dose equivalent overestimates the effective dose about 2.5 times.

These studies support the assumption that the ambient dose equivalent in practice does not underestimate the effective dose.

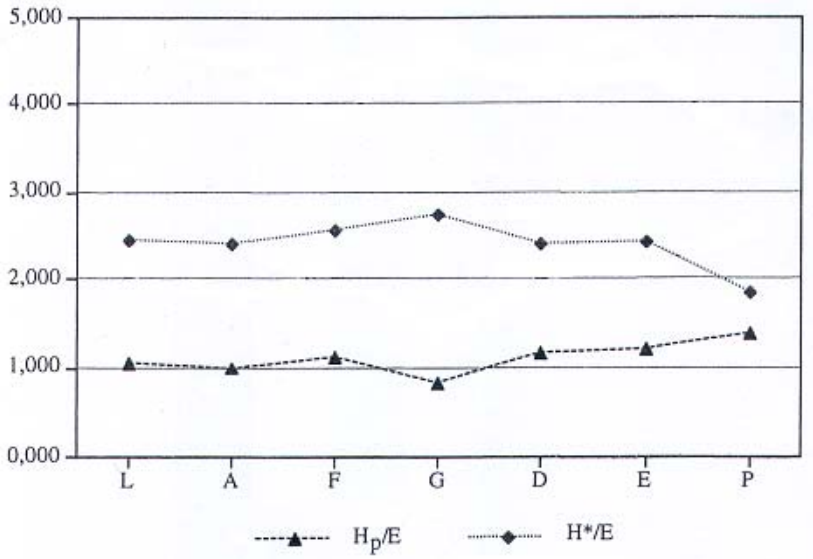

Figure 5. Experimental determinations of neutron dose equivalents in some positions of interest (L, A, F and G) at a nuclear power plant, and measurements around a transport container filled with spent nuclear fuel (D, E and P) [15].

3. Materials and Methods

Neutron measurements are difficult to perform due to the properties and type of interaction of the neutrons, and due to the fact that the neutrons have a wide energy distribution. The response of dosemeters varies considerably within this broad range. In general, neutron detectors give information only on the number of neutrons detected and not on their energy. Various types of detectors have been developed to detect neutrons in their different kind of energy regions. Most neutron detectors require some type of conversion of the incident neutron energy into charged, and thus, detectable particles. Some detectors also use the gamma rays produced by neutron capture reactions but these applications are rare [9] and such detectors have not been used in this work. Since neutron measurements only have been performed outside the treatment room, the problem with instruments which have long dead times and therefore tend to become saturated in pulsed radiation fields, is of less concern.

An important property of a neutron detector is the gamma ray sensitivity. It should either be insensitive to gamma rays or it should be able to distinguish the photon component. The cross section of a neutron reaction should be as large as possible, but the distance traveled by the reaction products is also significant. The active volume of the detector must be large enough to deposit all the kinetic energy of the rection products. This is easily achieved if the detection material is a solid because of the short range of the reaction products in solid but is more complicated if the detection material is a gas, where the ranges of the reaction products are typically several centimeters.

The calibration of the instruments is also important. A device calibrated in a reference neutron field will usually show results in the workplace differing from the true value. This deviation will depend on the difference between the neutron energy- and directional distribution of the reference and the workplace field [14].

The response of a measuring instrument needs to be taken into consideration. An ideal instrument for measuring the operational quantities would have a dose equivalent response independent of the energy and the direction of the incident neutron radiation [14].

For neutron measurements outside the shielded treatment room *active detectors* (BF_3 and ^3He proportional counters, semiconductor detectors) may be used but also *passive detectors* (bubble detectors, etch-track detectors) with high neutron sensitivities. Active detectors give an immediate readout and are usually used for short-term evaluation or warning in the case of raised radiation levels, while passive detectors are usually used for long-term exposure leading to a later evaluation of the measurement results [14]. Active detectors are designed to measure either dose equivalent (instruments usually called "rem-meters") or fluence (fluence meters). Neutron rem-meters are useful in situations where the neutron spectrum is unknown or poorly characterized, since their response is designed to be proportional to the dose equivalent. The rem-meter's response function is shaped to fit an appropriate fluence to dose-equivalent conversion function over a particular energy range. To follow the ICRP 1990 [13] effective dose recommendations, the operational quantity suitable for rem-meter calibration is ambient dose equivalent, *H*(10)*, which is defined as [16]:

$$H^*(10) = \int h_\Phi(E)\Phi(E)\,dE\,, \tag{3}$$

for a known neutron spectrum. $h_\Phi(E)$ is the fluence to ambient-dose-equivalent conversion function and $\Phi(E)$ is the neutron fluence as a function of energy for a given neutron field. The rem-meter response (R) in that field is given by equation (4):

$$R = \int C\, d_\Phi(E)\Phi(E)\,dE\,, \tag{4}$$

where $d_\Phi(E)$ is the response function of the rem-meter in units of counts per unit fluence and C is the calibration factor in units of sievert per count. The ratio $d_\Phi(E)/h_\Phi(E)$ defines the traditional energy response of the rem-meter in terms of counts per unit dose equivalent. The rem-meter measurement is considered to be accurate as long as $d_\Phi(E)$ has a similar energy response to that of $h_\Phi(E)$. The main problem is that $d_\Phi(E)$ does not fit $h_\Phi(E)$ over the entire energy range, so that some detectors tend to either under-respond or over-respond in certain energy regions. Therefore it is recommended to have some knowledge of the neutron spectrum in which measurements are to be made before any reliance can be placed on the instrument readings.

The neutron detectors/dosemeters used in this projekt are *area monitoring devices*: FHT 752 BF_3 neutron proportional counter from Thermo Eberline and LB 6411 ^3He neutron proportional counter from Berthold technologies; and *indvidual monitoring devices*: BD-PND bubble detectors, PADC neutron dosemeters and EPD-N2 electronic personal dosemeters.

3.1 Area monitoring devices

The BF_3 and ^3He proportional counters are hand-held area monitoring instruments whose reading is meant to be proportional to the ambient dose equivalent, *H*(10)*. They are active detectors constructed with a central thermal-neutron detector surrounded by a hydrogenous moderator where neutrons with higher energies are "thermalized". The energy response of a

moderated detector is mainly determined by its size and geometrical configuration. The thickness of the moderator is chosen to optimise the response as a function of energy.

3.1.1 Thermo Eberline ESM FH 40 G-L10 with FHT 752 neutron probe

The FH 40 G-L10 dose rate measuring unit is used for measuring ambient dose equivalent, *H*(10)*, of gamma- and x-rays with a proportional counter tube as detector. However the unit can be combined with various external probes to enhance the functionality of the unit and measure different radiation types. Neutron radiation can be measured with the FHT 752 Biorem BF_3 neutron probe.

The FHT 752 Biorem neutron probe (see figure 6) is a proportional counter tube filled with borontrifluoride (BF_3) where the gas is highly enriched in ^{10}B. The BF_3 proportional tube is designed for measuring ambient dose equivalent, *H*(10)*, and is widely used to detect slow neutrons due to the high detection efficiency for thermal neutrons. The gas is surrounded by a cylindrical hydrogenous moderator material of polyethylene and boron-carbide, where the fast and intermediate neutrons are slowed down. The BF_3 proportional detector has an extremely high gamma suppression if the photon fluence is not too high (as is the case for measurements outside the treatment room), so the neutron-induced events are of much larger amplitude than pulses generated by gamma ray background and are therefore easily detected. When a thermal neutron is absorbed by the ^{10}B component of the gas, an alpha particle and a recoil ^{7}Li nucleus are produced that travel off in opposite directions and create ion pairs. The nuclear reactions that take place are [9]

$$n + {}^{10}B \rightarrow {}^{7}Li + \alpha + 2.792\,MeV \quad \text{(ground state)}$$
$$n + {}^{10}B \rightarrow {}^{7}Li^{*} + \alpha + 2.310\,MeV \quad \text{(excited state)}$$

The recoil ^{7}Li nucleus can be left either in the ground state (about 6 % of the time) or an excited state (about 94 % of the time). The excited lithium nucleus quickly decays by emitting a 480 keV gamma ray which is usually lost from the detector.

One disadvantage with the BF_3 detector is its relative long time constant at low count rates, which makes neutron background measurements difficult to perform. However, this problem is of less concern for higher count rates.

Figure 6. The FHT 752 Biorem BF_3 neutron probe.

The thermal neutron cross section for the $^{10}B(n,\alpha)\ ^{7}Li$ reaction is 3840 barns. The cross section is strongly dependent on the incident neutron energy [7, 9]. It is decreasing with increasing neutron energy and is roughly proportional to *1/v* where *v* is the neutron velocity (see figure 8).

Due to the fact that the (n,α) reaction cross section of ^{10}B is so large at thermal energies, boron is usually used in neutron shielding materials [7]. This detector is commonly used for measurements outside the radiotherapy treatment room because it has a high photon suppression.

Some properties of the FHT 752 Biorem neutron detector according to the manufacturer are:

- Quantity: *H*(10)* for neutrons.
- Cylindrical moderator.
- Measuring range: 0- 0.4 Sv/h; neutron dose rate equivalent.
- Neutron energy range: 0.025 eV - 20 MeV according to ICRP 1990.
- Energy response: (see figure 9)
- Neutron response: 0.526 cps per μSv/h for ^{252}Cf.
- Gamma response: $< 10^{-8}$ cps at 1 mSv/h, so a discriminating neutron measurement can be performed in mixed fields.

The unit can be connected to a PC via an infrared connection using a special software such as FH40G.EXE. The functions available in the software and the measuring unit are explained in appendix II.

3.1.2 The LB 6411 Neutron probe from Berthold Technologies

The LB 6411 neutron probe (see figure 7) is a proportional counter tube filled with ^{3}He gas. It is designed for measuring ambient dose equivalent, *H*(10)*. The counter tube is surrounded by a spherical moderator of polyethylene. On top of the neutron probe is the LB123 Umo display unit. The nuclear reaction that take place in the detector is [9]

$$n + {}^{3}_{2}He \rightarrow {}^{3}_{1}He + p + 0.765\,MeV$$

The triton nucleus and the proton share the 765 keV reaction energy. The thermal neutron cross section for the ${}^{3}_{2}He(n,p){}^{3}_{1}He$ reaction is 5330 barns (much higher than for the boron reaction) and as for the $^{10}B(n,\alpha)\ ^{7}Li$ reaction, the cross section is strongly dependent on the incident neutron energy [7, 9] (see figure 8). The lower Q-value of the ^{3}He reaction makes gamma ray discrimination more difficult than for the BF_3 tube.

Figure 7. The LB 6411 ^{3}He neutron probe.

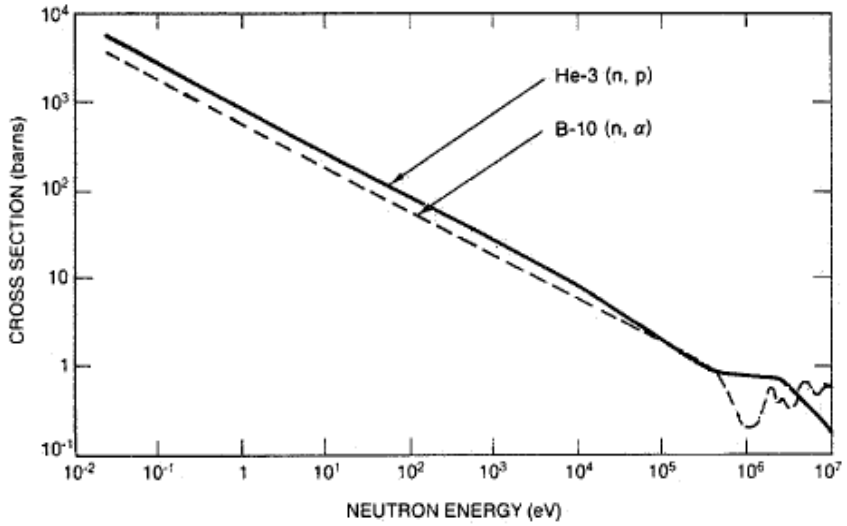

Figure 8. ^{10}B(n,α) and ^{3}He(n,p) cross sections as a function of neutron energy [17].

The energy response of the LB 6411 ^{3}He neutron probe to the ambient dose equivalent is shown in figure 9. In the energy range between 50 keV and 10 MeV the maximum deviation of the energy-dependent response relative to the calibration in a ^{252}Cf beam is ± 30%. The energy response of the FHT 752 BF_3 neutron probe is also shown in figure 9. As can be seen the BF_3 neutron detector is more sensitive than the ^{3}He neutron detector by a factor of two, from about 100 keV to 5 MeV, which is a possible explanation of the results later.

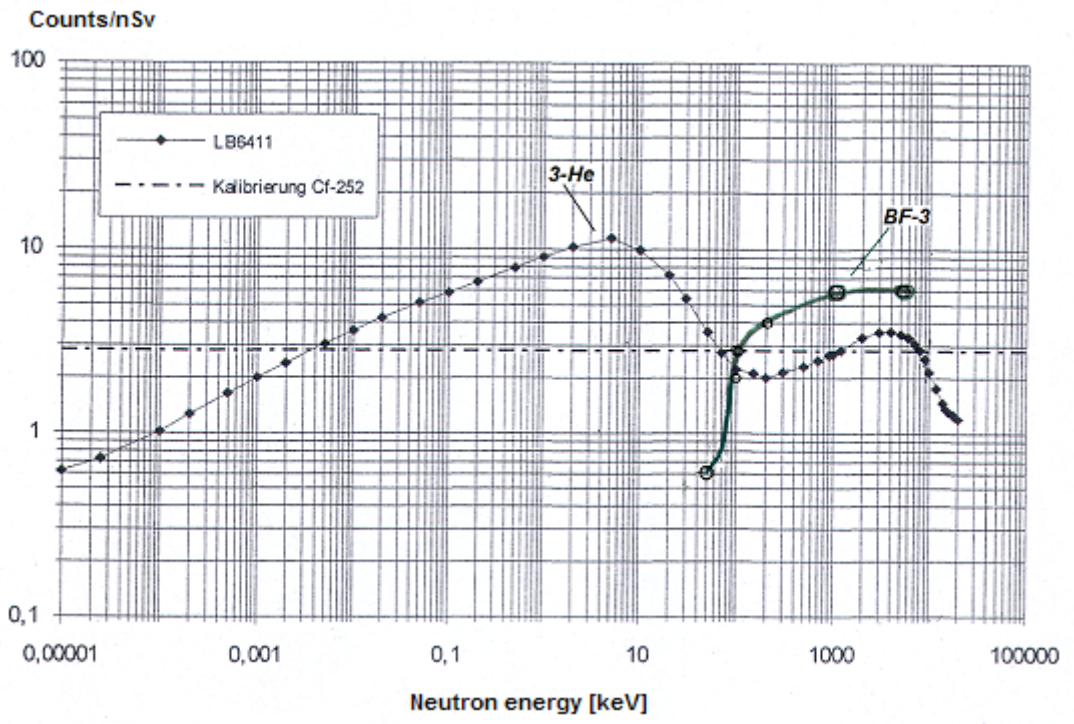

Figure 9. Energy response of the LB 6411 ^{3}He and the FHT 752 BF_3 neutron probe (according to the manuals of the manufactures). The calibration factor of the LB 6411neutron probe is illustrated by the dashed line and represents an acceptable response (i.e. over and under estimation balance) over the whole wide energy range of interest.

The calibration factor can be changed by the user to suit particular neutron fields. The ^{3}He neutron probe in this study is calibrated against the ^{241}Am-Be neutron source.

Due to the spherical geometry of the ^{3}He neutron probe there is no angular dependence of the sensitivity. Some properties of the LB 6411 neutron probe according to the manufacturer are:

- Quantity: *H*(10)* for neutrons.
- Spherical moderator.
- Measuring range: 100 nSv/h - 100 mSv/h; neutron dose rate equivalent.
- Neutron energy range: 0.025 eV - 20 MeV .
- Energy response: in the energy range between 50 keV - 10 MeV, ± 30% maximum deviation (see figure 9).
- Neutron response: 0.787 cps per µSv/h for ^{241}Am-Be.
- Gamma response: < 3 cps at 1 mSv/h in ^{137}Cs field.

3.2 Individual monitoring devices

The BD-PND bubble detectors, PADC neutron dosemeters and EPD-N2 electronic personal dosemeters are individual monitoring devices that measure personal dose equivalent, $H_p(10)$.

3.2.1 Bubble detectors

The neutron bubble detectors used in this project were a BD-PND (Bubble Detector - Personal Neutron Dosemeter) from Bubble Technologies Industries (BTI) in Canada (see figure 10). They are reusable, tissue equivalent integrating, passive dosemeters that provide immediate visible detection and measurement of neutron dose.

Figure 10. The BD-PND bubble detectors [18].

A bubble detector consists of a tube filled with an elastic polymer that contains almost invisible tiny droplets of superheated liquid (i.e. a liquid at a temperature above its normal boiling point). When a neutron strikes a droplet it can interact with the nucleus inside or near the droplet. The resulting secondary charged particles transfer energy to the droplet so that the liquid vaporizes and forms a visible gas bubble that is trapped inside the gel (see figure 11).

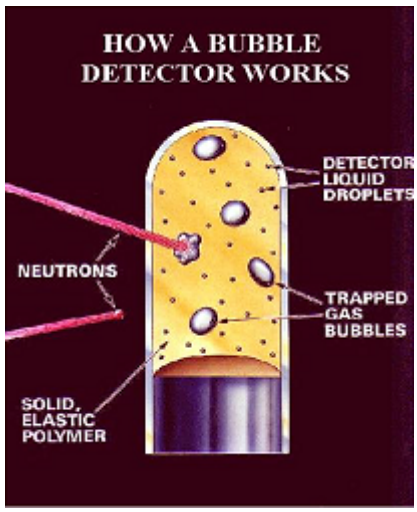

Figure 11. How a bubble detector works [18].

The number of accumulated bubbles can be counted by eye (for small numbers of bubbles) and is directly proportional to the personal dose equivalent. The detector may be reused and reset manually by screwing down a piston cap on top of the detector. This will increase the pressure that causes the bubbles to recondense. After about 10 to 20 cycles the bubbles may no longer recondense [14]. The number of reuses will affect the readings as well as the storage time and temperature before irradiation, and the time between irradiation and reading. The detector response as a function of neutron energy depends strongly on the temperature but is independent of dose rate. The energy response of the BD-PND to the personal dose equivalent

is shown in figure 12. From the threshold approximately 100 keV to about 300 keV the dose-equivalent response is fairly steep, but from about 200 keV to over 15 MeV the dose-equivalent response is reasonably flat.

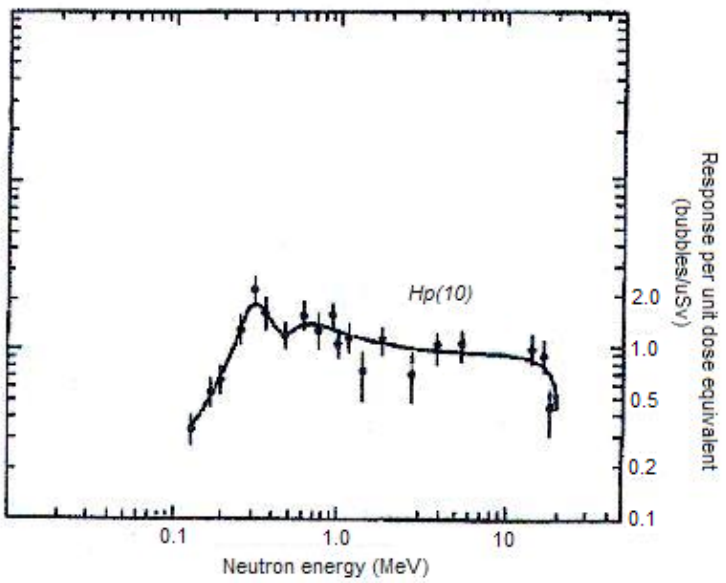

Figure 12. BD-PND energy response [18].

The recommended bubble detector for personal neutron dosimetry, according to the manufacturer, is the BD-PND. It is a temperature-compensated bubble detector so that no temperature corrections are required. The bubble detectors have an isotropic angular response and zero gamma sensitivity.

Some properties of the BD-PND detectors used in this study according to BTI are:

- Quantity: $H_p(10)$ for neutrons.
- Energy range: < 200 keV to > 15 MeV
- Dose range: 0.01 – 50 μSv
- Average sensitivity: 1.7 – 1.9 bubbles/μSv (average response between 20 – 37 °C)
- Optimum temperature range: 20 – 37 ºC

The sensitivity varies from detector to detector and depends on the number and size of the droplets, the atomic composition of the superheated droplets and the temperature and pressure of the surrounding medium [14]. To determine the BD-PND's detection sensitivity they are calibrated at BTI by exposing them to the ^{241}Am-Be neutron source under the temperature range 20 – 37 °C.

3.2.2 PADC Neutron Dosemeter

The PADC (polyallyl diglycol carbonate) neutron dosemeters (figure 13) used in this study are one of the approved dosimetry services offered by the Health Protection Agency (HPA), UK. The PADC dosemeter is a so-called etched-track detector [14] and a passive device that is able to detect neutrons over a wide energy range. It is insensitive to other radiations (gamma,

X-rays and betas) and is relatively unaffected by environmental factors such as heat and humidity. It also has a low radon sensitivity.

The PADC dosemeter is in the form of a clear plastic that is inside a holder. Incident fast neutrons with energies above about 150 keV and upwards interact with nuclei (by elastic scattering) in the dosemeter/holder assembly, while thermal neutrons interact with nitrogen nuclei in the holder. From these interactions charged particles (mostly protons) are produced. The charged particles damage the surface of the detector which leaves concealed tracks in the PADC (figure 14). By a suitable etching process, such as chemical etching and subsequent electrochemical etching, the damage tracks can be enlarged and form pits with a diameter of 20-200 μm. The number of pits is then determined in an automated reader that can be related to the personal dose equivalent. The efficiency of the etch and read procedures depends on particle type, their energy and angle of incidence. PADC etched-tracked detectors are suited for most workplaces where neutron radiation is present. In workplaces where there are significant contributions of the personal dose equivalent in the energy region between a few keV and about 100 keV special corrections must be applied [14].

Figure 13. The PADC dosemeter [19].

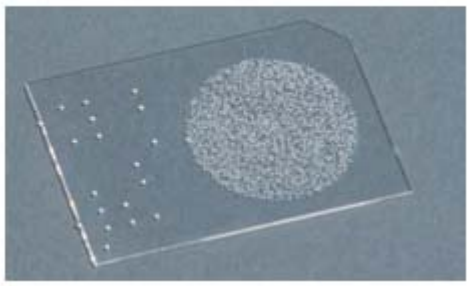

Figure 14. The etched plastic [19].

According to the manufacturer some properties of the PADC neutron dosemeters used in this study are:

- Quantity: $H_p(10)$ for neutrons.
- Energy range: thermal, epithermal (a few keV) and fast (144 keV to 15 MeV) neutrons
- Dose range: 0.2 – 250 mSv

The angular dependence of response is acceptable for the above energy range. The dosemeter has high sensitivity and does not have serious fading problems of the damage tracks. The energy response for fast neutrons is given for the quantity personal dose equivalent, $H_p(10)$, in figure 15 and is normalised to ^{252}Cf.

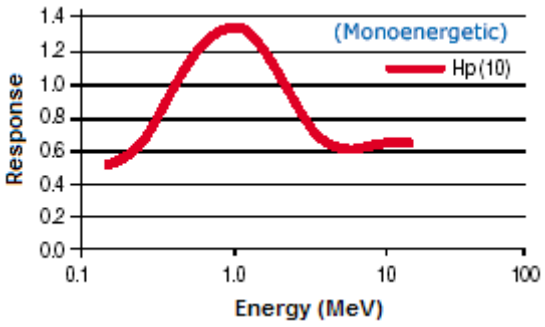

Figure 15. PADC energy response normalised to ^{252}Cf [19].

3.2.3 EPD-N2 Electronic Personal Dosemeter

The EPD-N2 is an active personal electronic dosemeter from Thermo Electron Corporation (see figure 16) that detects neutron and gamma radiation and gives a direct display of the radiation dose received by the wearer via a LCD display. The dosemeter is appropriate for workplaces with mixed gamma/neutron fields. The neutron and photon (gamma/x-ray) components are displayed and stored separately.

Figure 16. EPD-N2 personal electronic dosemeter [20].

The EPD-N2 contains multiple silicon diode detectors. The detectors are semiconductors and because silicon detectors have little intrinsic sensitivity to neutrons, they require special converter layers to be able to detect the neutrons. The EPD-N2 uses two special materials, a polymer layer that generates knock-on protons from fast neutrons, and a ^{6}LiF layer that generates high-energy alpha particles and tritons from the ^{6}Li(n,α)^{3}H reaction [21]. The outputs from the detectors are combined using suitable algorithms to estimate the personal dose equivalent, $H_p(10)$, and the dose equivalent rate. The neutron source that has been used for calibration is ^{241}Am-Be. The neutron detectors are much less sensitive than the photon detectors in terms of counts detected per uSv of radiation dose. Thus the statistical accuracy and hence the dose rate response for neutron dose are worse than those for photon dose.

Some properties of the EDP-N2 dosemeter according to the manufacturer are:

- Quantity: $H_p(10)$ for photons and neutrons.
- Energy range: 25 keV to >7 MeV (photon) ; thermal to >15 MeV (neutron)
- Dose display and storage: 0 µSv to >16Sv (auto ranging)
- Neutron angular response: $H_p(10)$ (n) ± 50% up to ± 75%
- Neutron energy response: (see figure 17)

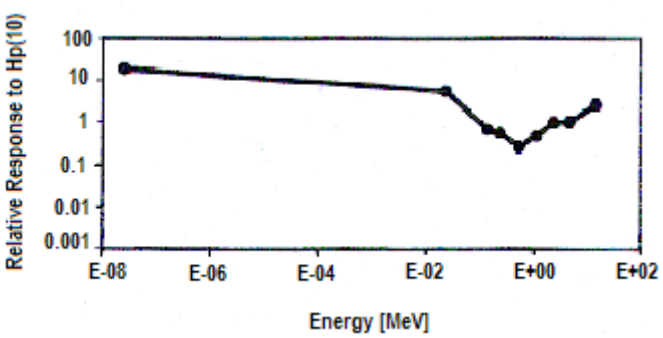

Figure 17. EPD-N2 neutron energy response (according to the manual of the manufacturer).

The functions of the EPD-N2 can be configured via an infrared interface using a suitable software such as EasyEPD2 (see appendix II).

3.3 The radiotherapy unit at UMAS

At UMAS there are two linear accelerators that operate above 10 MV: Varian Clinac 2100C/D and Elekta precise. Varian is capable of producing 6 and 18 MV x-ray beams and 6, 9, 12, 16 and 20 MeV electron beams. This linac is denoted as L22. Elekta is capable of producing 6, 10 and 18 MV x-ray beams and 6, 8, 10, 12 and 18 MeV electron beams. This linac is denoted as L12. Figure 18 shows the radiotherapy unit at UMAS. The pointing direction for gantry angle 90º and 270º is also illustrated. With gantry angle 0º and 180º the beam is directed downwards and upwards respectively. The bunkers of the two linacs differ in size and construction. The main difference (in neutron-shielding point of view) between the bunkers is their door materials. The door of L22 contains 70 mg/cm^2 boron, 100 mm paraffin and 6 mm steel, while the door of L12 contains 4 mm lead and 4 cm boron polyethylene (8% B_4C).

To make an understanding of how the patient treatments with high-energy photon beams are distributed at the two accelerators, statistics have been kept almost every day for about two months over the number of patients and high-energy-photon fields (see section 4.2).

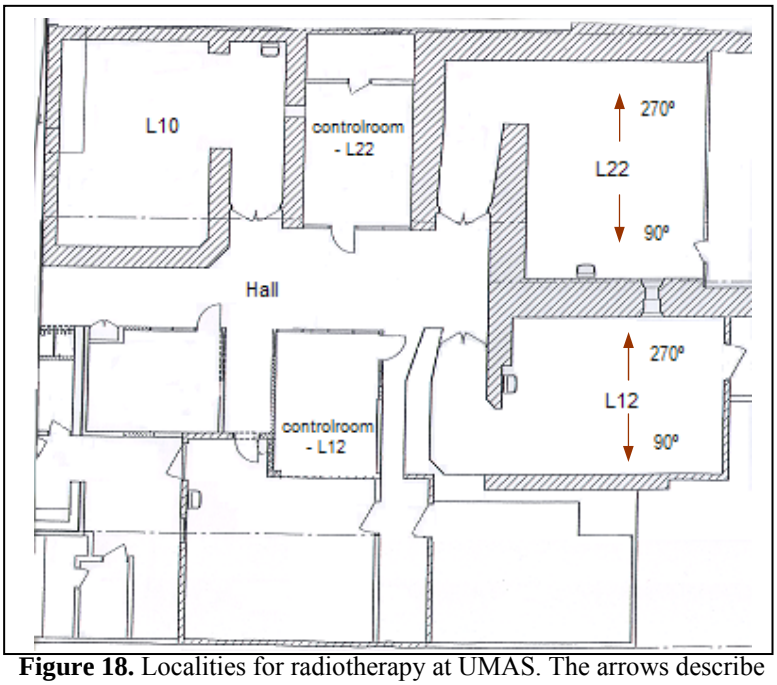

Figure 18. Localities for radiotherapy at UMAS. The arrows describe the pointing direction for gantry angle 90º and 270º.

3.4 Measurements with the area monitoring devices

Measurements with the FHT 752 BF_3 and the LB 6411 ^3He neutron probes were made in experimental form to make a survey of the neutron dose rate around the radiotherapy facility. Measurements with the BF_3 detector were also performed when the accelerators were in clinical use during patient treatment. For measurements inside the control room the detectors were placed on the floor in the centre of the room. For all measurements with the BF_3 detector the sampling interval was chosen to 5 seconds.

Three phantoms were used in this study: phantom 1 = solid water phantom (30*30*15 cm^3), phantom 2 = anthropomorphic phantom (Alderson), phantom 3 = PMMA phantom (30*30*12 cm^3).

3.4.1 Experimental measurements

Measurements with the BF_3 detector inside the control room and outside the treatment door of L12.

Phantom 1 was irradiated with high-energy photons with gantry angle 0°, 90°, 180° and 270° to study the neutron dose rate in the control room of L12. Three different energies 6, 10 and 18 MV and two different field sizes, (10*10 cm^2) and (30*30 cm^2) respectively, were investigated. The linac settings are presented in table 1.

For measurements outside the treatment door of L12, phantom 2 was irradiated with photon energy 18 MV, gantry angle 270° and field size (15*15 cm^2). The settings are presented in table 2.

Table 1. L12 settings during phantom 1 irradiation with the BF_3 detector inside the control room of L12. The approximate time when starting the measurement is also given.

Time [hh:mm]	**Energy** [MV]	**Field size** [cm]	**Gantry angle**
14:08	6	10*10	0º
14:12	10	10*10	0º
14:18	18	10*10	0º
14:22	6	30*30	0º
14:29	10	30*30	0º
14:35	18	30*30	0º
14:43	10	10*10	90º
14:50	18	10*10	90º
14:56	10	30*30	90º
15:00	18	30*30	90º
15:06	10	10*10	180º
15:14	18	10*10	180º
15:19	10	30*30	180º
15:26	18	30*30	180º
15:33	10	10*10	270º
15:40	18	10*10	270º
15:43	10	30*30	270º
15:48	18	30*30	270º

Table 2. L12 settings during phantom 2 irradiation with the BF_3 detector outside the treatment door of L12.

Energy [MV]	**Field size** [cm]	**Gantry angle**
18	15*15	270º

Measurements with the BF_3 detector inside the control room and outside the treatment door of L22.

For neutron measurements inside the control room of L22 phantom 2 was irradiated with 18 MV photon beams with gantry angle 0°, 90°, 180° and 270°, and field size (15*15 cm^2). One measurement with a dynamic wedge of 60° was also investigated. The neutron dose rate with high-energy electrons (12 MeV and 20 MeV) was studied for gantry angle 0° and field size (15*15 cm^2). The settings are presented in table 3.

The linac settings for neutron measurements outside the treatment door of L22 were: photon energy 18 MV, gantry angle 0° and field size (15*15 cm^2). For this measurement phantom 2 was used. The settings are presented in table 4.

Table 3. L22 settings during phantom 2 irradiation with the BF_3 detector inside the control room of L22. The approximate time when starting the measurement is also given.

Time [hh:mm]	**Energy**	**Field size** [cm]	**Gantry angle**
16:07	18 MV	15*15	0º
16:09	18 MV	15*15	0º
16:16	18 MV	15*15	0º
16:22	18 MV	15*15	90º
16:28	18 MV	15*15	270º
16:36	18 MV	15*15	180º
16:48	12 MeV	15*15	0º
16:48	20 MeV	15*15	0º
16:55*	18 MV	15*15	0º

* Dynamic wedge 60º.

Table 4. L22 settings during phantom 2 irradiation with the BF_3 detector outside the treatment door of L22.

Time [hh:mm]	**Energy** [MV]	**Field size** [cm]	**Gantry angle**
16:41	18	15*15	0º

Measurements with the BF_3 and ^{3}He detectors around the radiotherapy facility of L12 and L22.

Experimental measurements were performed with the BF_3- and ^{3}He detectors around the radiotherapy facility of L12 and L22. A photon measuring device was also used to compare the neutron- with the photon dose rate. Figure 19 shows the positions of the detectors (marked with figures) and table 5-7 present the linac settings during the exposures. At position 1-11, measurements were performed while irradiating phantom 2 in L12, position 12-14 while irradiating phantom 3 in L22, and position 15-17 while irradiating from both linacs at the same time.

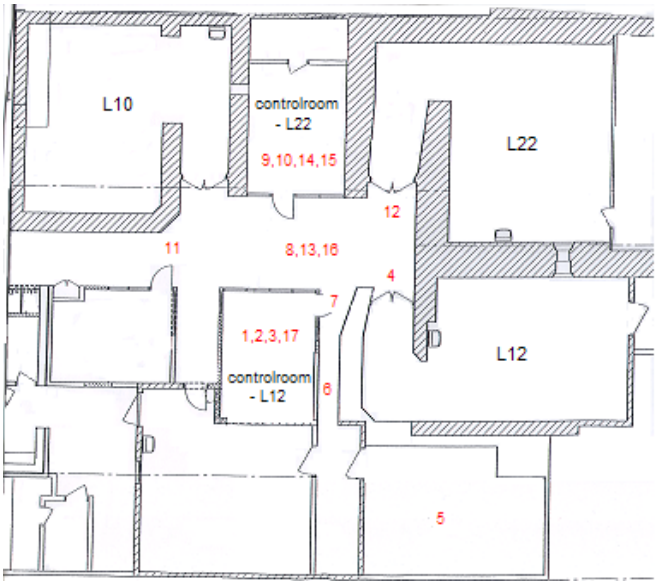

Figure 19. The positions (marked with figures) of the BF_3- and ^{3}He-detectors during the measurements around the radiotherapy facility.

Table 5. L12 settings during phantom 2 irradiation, with the BF_3- and ^3He detectors around the radiotherapy facility.

Position	Energy [MV]	Field size [cm]	Gantry angle
1.	18	15*15	0º
2.	18	15*15	0º
3.	18	15*15	270º
4.	18	15*15	270º
5.	18	15*15	270º
6.	18	15*15	270º
7.	18	15*15	270º
8.	18	15*15	270º
9.	18	15*15	270º
10.	18	15*15	0º
11.	18	15*15	0º

Table 6. L22 settings during phantom 3 irradiation, with the BF_3- and ^3He detectors around the radiotherapy facility.

Position	Energy [MV]	Field size [cm]	Gantry angle
12.	18	15*15	0º
13.	18	15*15	0º
14.	18	15*15	0º

Table 7. L12 and L22 settings during phantom irradiation at the same time, with the BF_3- and ^3He detectors around the radiotherapy facility. Phantom 2 was used in L12, and phantom 3 was used in L22.

Position	Linac	Energy [MV]	Field size [cm]	Gantry angle
15-17.	L12	18	15*15	0º
15-17.	L22	18	15*15	0º

3.4.2 Measurements during patient treatment

Neutron measurements were made during patient treatment for a whole workday with the BF_3 detector placed on the floor in the centre of the control room in L12 and L22 respectively. Before the start of patient treatments, a morning control, i.e. a warm up of the accelerator and a daily control of the absorbed dose, is always done.

Measurements with the BF_3 detector inside the control room of L12 during morning control and patient treatment.

The linac settings during the morning control of L12 are presented in table 18 in appendix III. At this measurement day (2005.11.30) 16 patients were treated in L12 whereas 5 of them (a total of 9 fields) were treated with 10 MV photons and 5 (a total of 7 fields) with 18 MV photons. The linac settings during these treatments with high-energy photons are presented in table 19 in appendix III.

Measurements with the BF_3 detector inside the control room of L22 during morning control and patient treatment.

The linac settings during the morning control of L22 are presented in table 20 in appendix III. At this measurement day (2005.11.29) 22 patients were treated in L22, all of them with 18 MV photons (a total of 68 fields). The linac settings during these treatments with high-energy photons are presented in table 21 in appendix III.

3.5 Measurements with the individual monitoring devices

Measurements with the BD-PND bubble detectors, EPD-N2 electronic personal dosemeters and PADC neutron dosemeters were performed by letting the personnel, one from L12 and one from L22, carry all the devices during their time of work. The personal dosemeters were alternated between individual staff members from the same linac, so that all the dosemeters were always carried by one individual.

3.5.1 Measurements with the BD-PND bubble detectors

The two bubble detectors in this study were carried by the personnel, one from L12 (with an average sensitivity of 1.8 bubbles/μSv) and one from L22 (with an average sensitivity of 1.7 bubbles/μSv), during their time of work for a period of 12 workdays. The number of bubbles were counted every day.

3.5.2 Measurements with the EPD-N2 electronic personal dosemeters

The two electronic personal dosemeters in this study were carried by one person from L12 and one from L22, during their time of work for a period of 1 month (22 workdays). The dosemeters were switched on all the time, including weekends. At the end of the workday they were placed in the personnel's locker-room away from the linacs. Hence the total accumulated dose that the dosemeters show after one month is not just the dose received by the personnel during their time of work, but also due to background radiation during non-working hours. Since the dosemeters store the dose values, the dose received every day can be viewed via the EasyEPD2 software (see appendix II).

3.5.3 Measurements with the PADC neutron dosemeters

Two PADC dosemeters in this study were carried by one person from L12 and one from L22, during their time of work for a period of one month. Two other PADC dosemeters were also placed at the wall in the control rooms against the linear accelerator in L22 and L12 respectively as a reference.

4. Results and Discussion

4.1 Measurements with the area monitoring devices

4.1.2 Experimental measurements

Measurements with the BF_3 detector inside the control room and outside the treatment door of L12 and L22.

The results from the BF_3 phantom measurements, with the detector placed inside the control room and outside the treatment door of L12 and L22 respectively are shown in figure 20-23 and in table 8. The linac settings during these measurements are presented in table 1-4 in section 3.4.1.

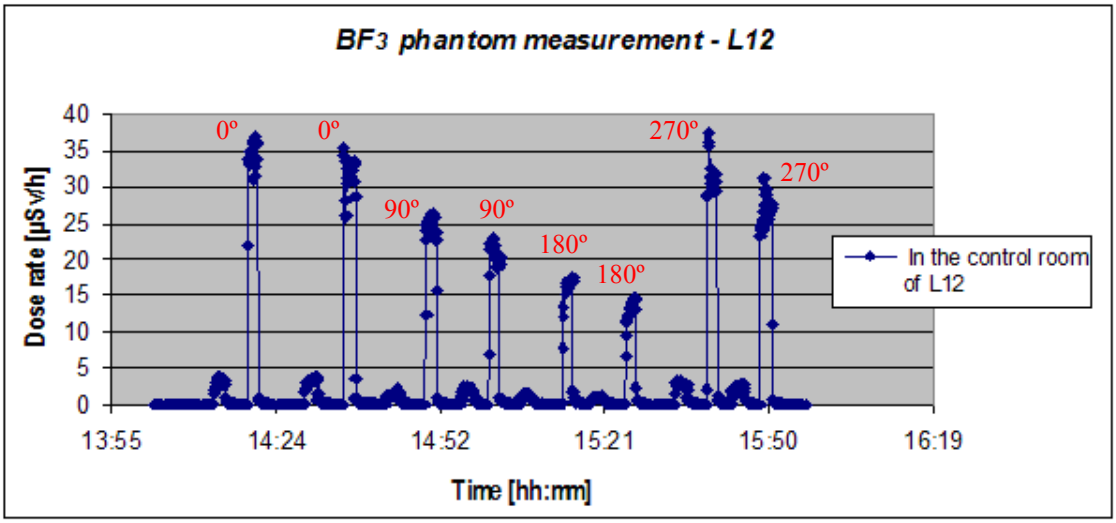

Figure 20. The neutron dose rate (*H*(10)*) from the measurements during phantom irradiation in L12, with the BF_3 neutron detector placed inside the control room. The highest peaks (above ~15 µSv/h) correspond to 18 MV photon beams. Figures at the peaks =gantry angle. (For linac settings see table 1 in section 3.4.1).

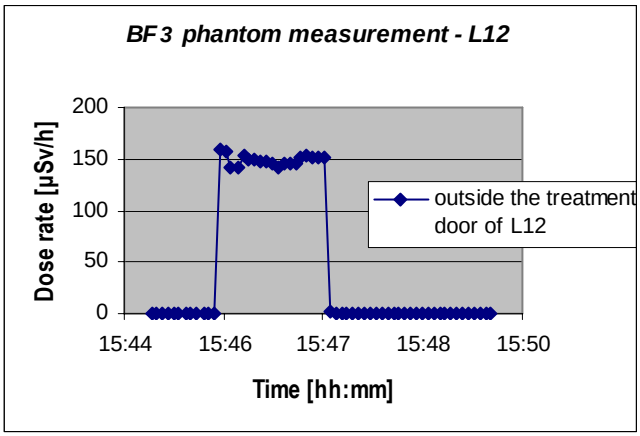

Figure 21. The neutron dose rate (*H*(10)*) from the measurements during phantom irradiation in L12 with 18 MV photon beams and with the BF_3 neutron detector placed outside the treatment door. (For linac settings see table 2 in section 3.4.1).

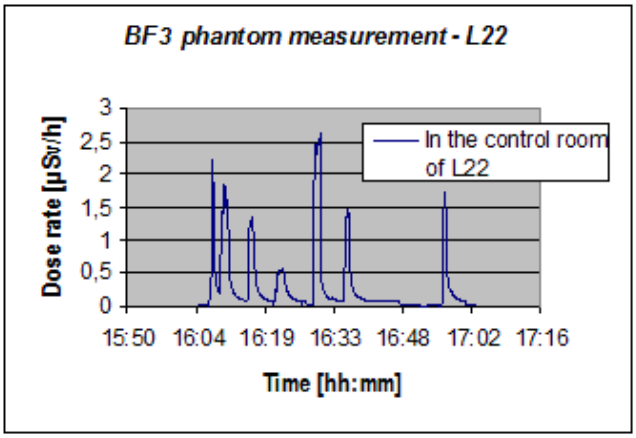

Figure 22. The neutron dose rate (*H*(10)*) from the measurements during phantom irradiation in L22, with the BF_3 neutron detector placed inside the control room. Gantry angle 270º (fifth peak from the left) showed the highest dose rate (2.5 µSv/h). (For linac settings see table 3 in section 3.4.1)

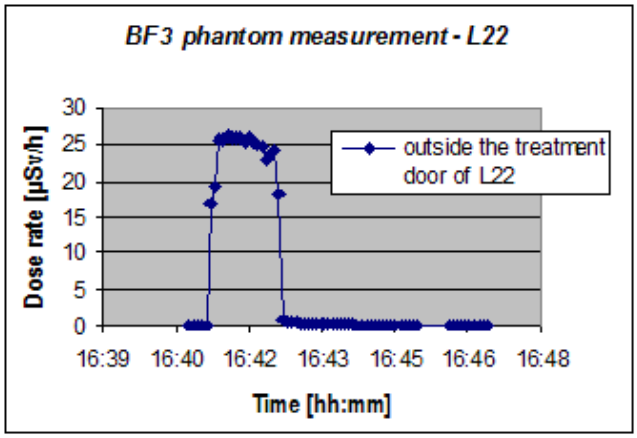

Figure 23. The neutron dose rate (*H*(10)*) from the measurements during phantom irradiation in L22 with 18 MV photon beams, and with the BF_3 neutron detector placed outside the treatment door. (For linac settings see table 4 in section 3.4.1).

As expected the highest neutron dose-rate peaks (above ~15 µSv/h) in figure 20 correspond to the use of 18 MV photon beams. The dose rate for the 10 MV and 6 MV photon beams was below about 5 µSv/h and 1 µSv/h respectively. Gantry angle 0º and 270º showed the highest dose rate (~30-35 µSv/h). Comparison between the two different field sizes (30*30 cm^2) and (10*10 cm^2) for gantry angle 0º and 180º didn't show any significant changes in dose rate. This is because the most important photoneutron sources are materials inside the linac head. With gantry angle 90º and 270º, the larger field size did not completely cover the phantom. Since photoneutron production also depends on any scattering material, to which the photon beam is incident, this could explain the lower dose rate values in this geometry compared to the smaller field size.

The highest neutron dose rate when using 18 MV photon beams during phantom irradiation in L12, was about 35-40 µSv/h inside the control room (figure 20) and about 150 µSv/h outside the treatment door (figure 21). When using 18 MV photon beams during phantom irradiation in L22, the highest dose rate was much lesser, about 2.5 µSv/h inside the control room (figure 22) and about 25 µSv/h outside the treatment door (figure 23).

In L22 gantry angle 270º showed the highest dose rate, about 2.5 µSv/h (figure 22). In accordance with the theory that the cross section for electronuclear reactions is much smaller than for photonuclear reactions, irradiation with high-energy electron beams didn't show any dose rate peaks. The dose rate values were about the same as for neutron background radiation (i.e. ~ 20 nSv/h).

The most important results from these measurements are that the neutron dose rate is much higher in the control room (where the personnel normally are staying during patient treatment) of L12 than in the control room of L22.

Similar measurements have been performed with the same BF_3 detector and at the same department in an earlier study in 2002 [22] that can be compared with the results of the present investigation. The earlier study showed that the neutron dose rate in the control room and outside the treatment door of L12 was about 35-40 µSv and 200 µSv respectively.

Measurements with the BF_3 and ^3He detectors around the radiotherapy facility of L12 and L22.

The results from the measurements with the BF_3 and ^3He detectors around the radiotherapy facility are presented in table 8. The position of the detectors and the linac settings during the exposures can be seen in figure 19 and table 5-7 in section 3.4.1.

Table 8. The neutron- and photon dose rate (*H*(10)*) at the different positions around the radiotherapy facility. The lines marked with, /, mean that no measurement was performed. $\bar{x}$ is the average value of the ratio. (The position of the detectors and the linac settings can be seen in figure 19 and table 5-7 in section 3.4.1).

	Neutron dose rate [μSv/h]			**Photon dose rate** [μSv/h]
Position	**BF_3**	**^3He**	**Ratio (BF_3/^3He)**	
1.	35	19	1.8	/
2.	35	17	2.1	/
3.	30	10	3	/
4.	150	66	2.3	50
5.	0.2	0.02	10	0.6
6.	20	5	4	/
7.	50	20	2.5	8
8.	90	40	2.3	20
9.	18	5	3.6	4.5
10.	19	8.5	2.2	4.5
11.	25	13	1.9	3
12.	13.5	6.5	2.1	70
13.	3.5	1.5	2.3	10
14.	2.5	0.8	3.1	0.5
15.	16	10	1.6	5
16.	90	45	2	25
17.	40	19	2.1	10
			$\bar{x} = 2.9$	

As can be seen from the results in table 8, the BF_3 detector measured neutron dose rates by a factor of 2-3 higher than the ^3He detector. One possible explanation to this is the different energy responses of the detectors (see figure 9), where the BF_3 detector is a factor of two more sensitive than the ^3He neutron detector in the interesting energy region from about 100 keV to 5 MeV. Other things that can influence the differences in the results are the different detector materials, detector designs and neutron responses. It could have been of interest to compare with a third area monitoring device.

Like previous phantom measurements with the BF_3 detector, irradiation in L12 showed higher neutron dose rates than irradiation in L22. The highest dose rates when irradiating the phantom in L12 was outside the treatment door of L12 (position 4), at the hallway between the two control rooms (position 8) and inside the control room of L12 (position 1, 2, 3). The neutron dose rate inside the control room of L12 during phantom irradiation in L12 was about

35 µSv/h for the BF_3 detector, in agreement with previous results (see figure 20). The neutron dose rate inside the control room of L22 was higher during irradiation in L12 (about 19 µSv/h) than during irradiation in L22 (about 2.5 µSv/h). The most important result is that in almost all positions, the neutron dose rate was higher than the photon dose rate when using 18 MV photons from L12.

The angular dependence was also studied by changing the position between the two neutron detectors (position 1-2) and with the same linac settings, but no particular changes occurred in the response of the detectors. At the first measurement (position 1) the neutron detectors were placed aside, and at the second measurement (position 2) their positions were switched.

4.1.3 Measurements during patient treatment

Measurements with the BF_3 detector inside the control room of L12 and L22 during morning control and patient treatment.

The results from the measurements during the morning control of the accelerator and patient treatments, with the BF_3 neutron detector, are shown in figure 24-27. The amount of gamma-, neutron- and total dose accumulated in the BF_3 detector during this time is shown in table 9-10. For linac settings see table 19-22 in appendix III.

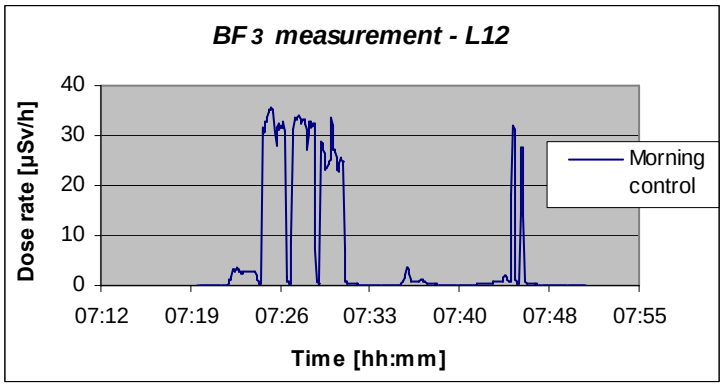

Figure 24. The neutron dose rate (*H*(10)*) from measurements with the BF_3 neutron detector placed inside the control room of L12 during the morning control of the accelerator. (For linac settings see table 19 in appendix III).

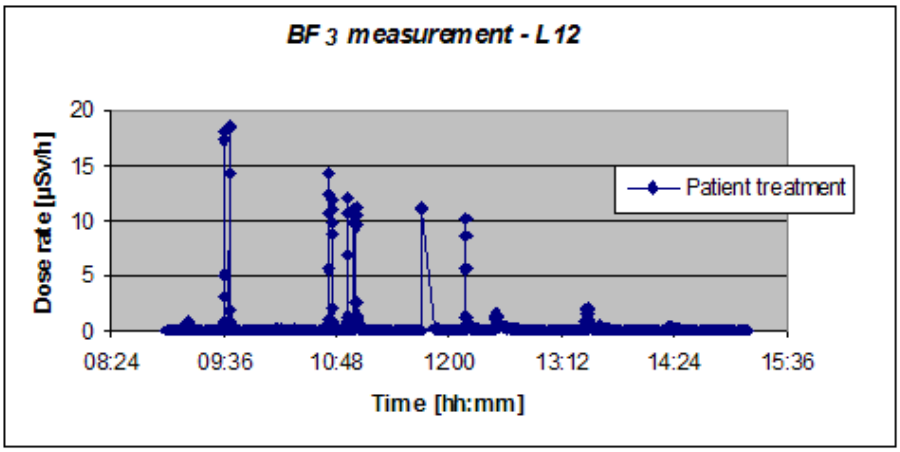

Figure 25. The neutron dose rate (*H*(10)*) from measurements with the BF_3 neutron detector placed inside the control room of L12 during patient treatment. (For linac settings see table 20 in appendix III).

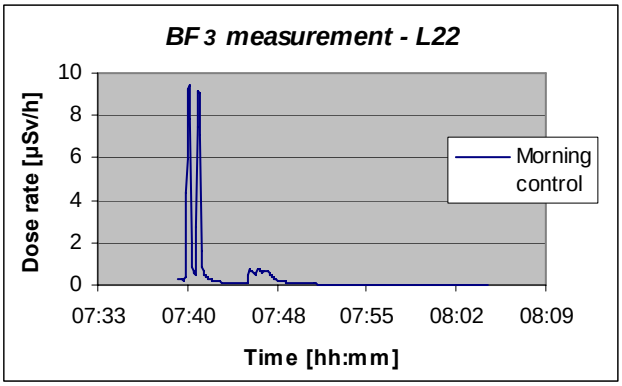

Figure 26. The neutron dose rate (*H*(10)*) from measurements with the BF_3 neutron detector placed inside the control room of L22 during the morning control of the accelerator. (For linac settings see table 21 in appendix III).

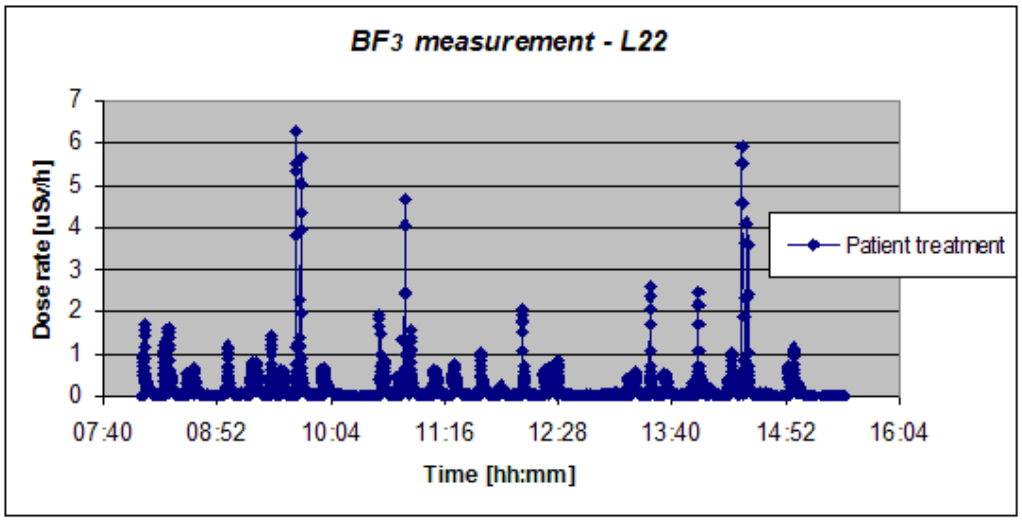

Figure 27. The neutron dose rate (*H*(10)*) from measurements with the BF_3 neutron detector placed inside the control room of L22 during patient treatment. (For linac settings see table 22 in appendix III).

Table 9. The amount of gamma-, neutron- and total dose accumulated in the BF_3 instrument during a whole workday in L12.

Dose	[µSv]
Gamma	2.1
Neutron	4.1
Total	6.2

Table 10. The amount of gamma-, neutron- and total dose accumulated in the BF_3 instrument during a whole workday in L22.

Dose	[µSv]
Gamma	1.1
Neutron	0.9
Total	2.0

In figure 24, the first small peak corresponds to 10 MV photon beam and the five highest peaks corresponding each to 18 MV photon beams. A small peak (between 7.30 and 7.40) also arised during irradiation with electron beams, probably from the highest energy (18 MeV). In figure 25, the three first peaks correspond to the first three patient treatments with 18 MV photon beams before lunch. There are some peaks during lunch, when there were no treatments, most likely because of some measurements and control of the linear accelerator at this day. After lunch there were two more 18 MV treatments that can not be seen in figure 25, probably because the received dose and dose rate at these treatments was too small for the detector to be registered.

The neutron dose rates in the control room during the morning control and patient treatments are much lower in L22 (figure 26 and 27) than in L12 (figure 24 and 25). In figure 27 there are some peaks that are higher than the other. Since there were no particular differences in linac settings between these treatments, the reason for this might be that there have been 18 MV treatments in L12 at the same time. There are some peaks also here during lunch, when there were no treatments, with the same explanation as for figure 25.

These measurements show that the highest neutron dose rates (about 35 µSv/h for L12 and 9 µSv/h for L22) arise during the morning control of the linac. This is because during morning control the total dose and dose rate is much higher than it normally is during patient treatment.

In L12 the neutron dose accumulated in the BF_3 instrument is higher than the gamma dose by a factor of 2. In L22 the gamma and neutron dose is about the same. Since the BF_3 detector was placed inside the control room all the time during the measurement, the accumulated dose in table 9 and 10 is also due to the measurements and controls of the linear accelerators that were performed during lunchtime.

4.2 Statistics

During the period 2005.09.29 – 2005.10.28 (i.e. 22 workdays), the number of 10 MV and 18 MV fields in L12 was 456 and 158 respectively and in L22 the number of 18 MV fields was 975. During the period 2005.11.08 – 2005.12.07 (i.e. 22 workdays), the number of 10 MV and 18 MV fields in L12 was 239 and 135 respectively and in L22 the number of 18 MV fields was 1501. Most of the 18 MV treatment fields are given in L22 due to the poorer shielding of neutrons in L12.

4.3 Worst case scenario

The maximum number of 18 MV fields at one day in L12 was 15. The highest neutron dose rate with the BF_3 measurements inside the control room of L12 during patient treatment was about 18 µSv/h. To make a rough approximation to the L12 personnel neutron doses the following assumptions are made:

Number of workdays per year: 200 days
Number of 18 MV fields per day: 15
Irradiation time per field: 1 minute
Irradiation time per year: 50 h

→ The accumulated neutron ambient dose equivalent during their time of work:
18 µSv/h*50 h = 900 µSv/year ≈ ***1 mSv/year***

4.4 Measurements with the individual monitoring devices

4.4.1 Measurements with the BD-PND bubble detectors

The number of bubbles formed each day is presented in figure 28-29.

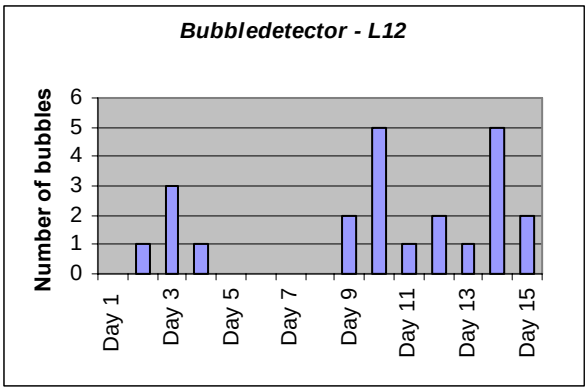

Figure 28. Number of bubbles each day in L12.

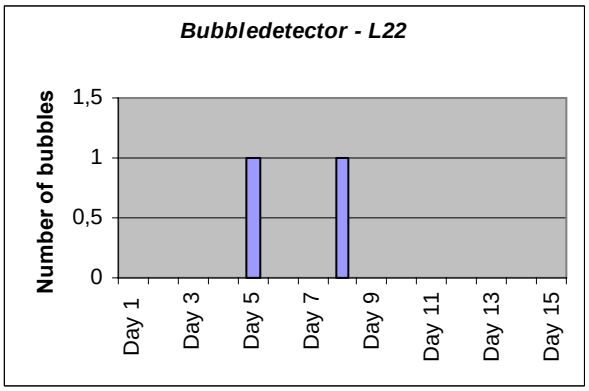

Figure 29. Number of bubbles each day in L22.

The bubble detectors were carried for a period of total 12 workdays. The neutron dose during this period can be calculated from the average sensitivities of the BD-PND's and the total number of bubbles counted. The neutron dose per workday can then be estimated by dividing the neutron dose with 12. These results are presented in table 11. The number of resets of the bubble detectors in L12 was about 8-10 and in L22 about 3-5.

Table 11. The estimated neutron dose during 12 and one workday respectively.

	Total number of bubbles	Average sensitivity [bubbles/µSv]	Neutron dose [µSv/12days]	Neutron dose [µSv/day]
L12	23	1.8	12.8	1.1
L22	2	1.7	1.2	0.1

Since the number of reuses will affect the readings, the number of bubbles formed each day was sometimes easier and sometimes more difficult to see. The total number of bubbles was only counted by one person. To decrease the uncertainty the total number of bubbles should be counted by two or more persons. The number of bubbles formed each day was varying depending on if that person performed the morning control or not, the number of 18 MV treatments that day, and their time at work. The neutron dose is higher in L12 than in L22 by a factor of about 10.

4.4.2 Measurements with the EPD-N2 Electronic Personal Dosemeters

Table 12 shows the amount of gamma-, neutron- and total dose accumulated in the EPD-N2 electronic personal dosemeters during one month (a total of 30 days including weekends) in L12 and L22. Via the EasyEPD2 software one can view the accumulated dose after each day. Figures 30-34 show the accumulated gamma and neutron dose after each working day (by assuming the time the personnel started and finished the work) and during weekends for one month. In some days the dosemeters showed surprisingly high figures late in the evening or during a weekend, when the personnel normally aren't at work. Figure 34 is a good illustration for this where the dose values lied around 1 μSv at three weekends except for one weekend where the dose value was 11 μSv. These sudden "dose changes" could just be observed for the neutron doses. Figures 35-36 show the dose profile that can be viewed via the EasyEPD2 software.

Table 12. The amount of gamma-, neutron- and total dose accumulated in the EPD-N2 during one month (a total of 30 days including weekends) in L12 and L22.

	L12	L22
Dose	[μSv]	[μSv]
Gamma	72	95
Neutron	111	82
Total	183	177

The results in table 12 can be compared with the gamma dose from TLDs. According to the monthly reported TLD values, the average gamma dose to the personnel working in L12 and L22 respectively during the same month as the EPD:s are:

Personnel in L12 (an average value from four persons): 0.05 mSv per month and person
Personnel in L22 (an average value from four persons): 0.08 mSv per month and person

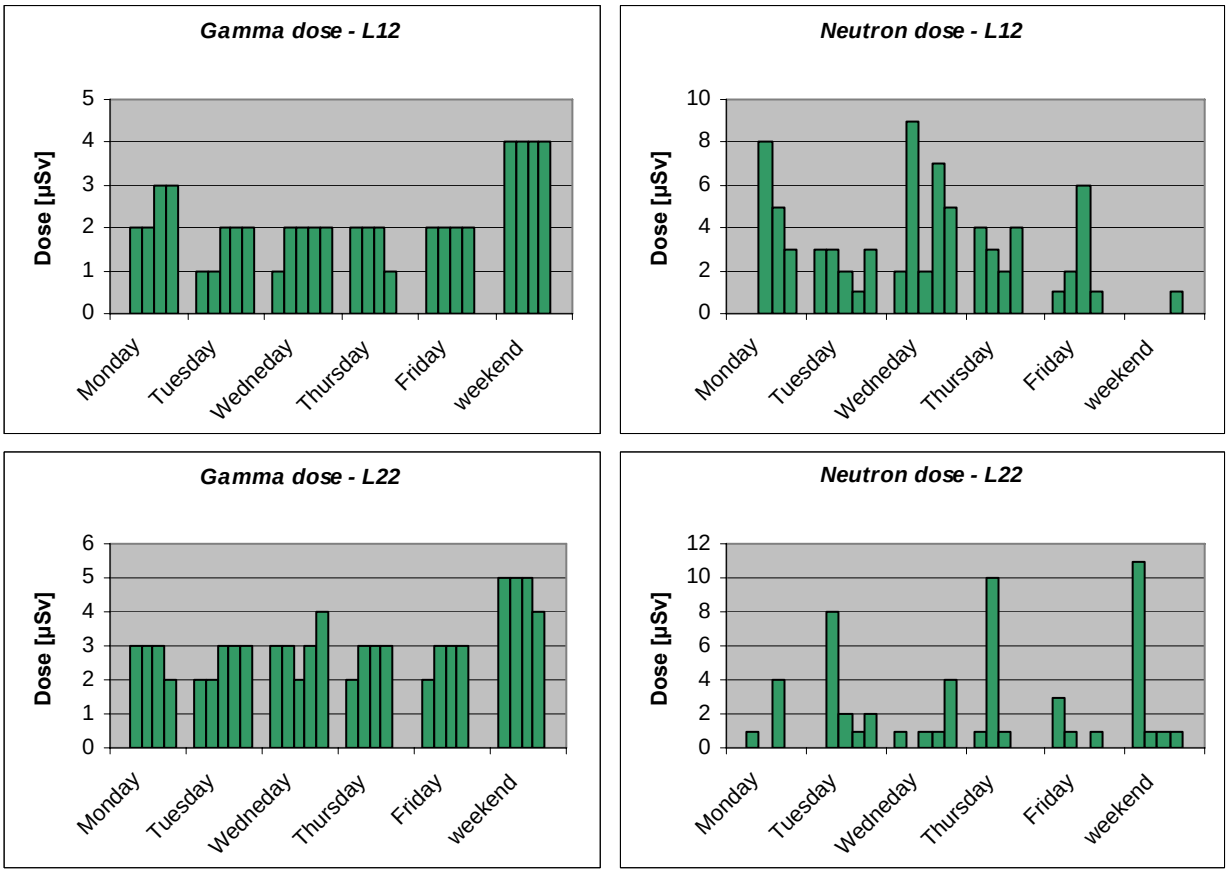

Figure 30-34. The accumulated gamma and neutron dose in the EPD-N2 after each working day and during weekends in one month.

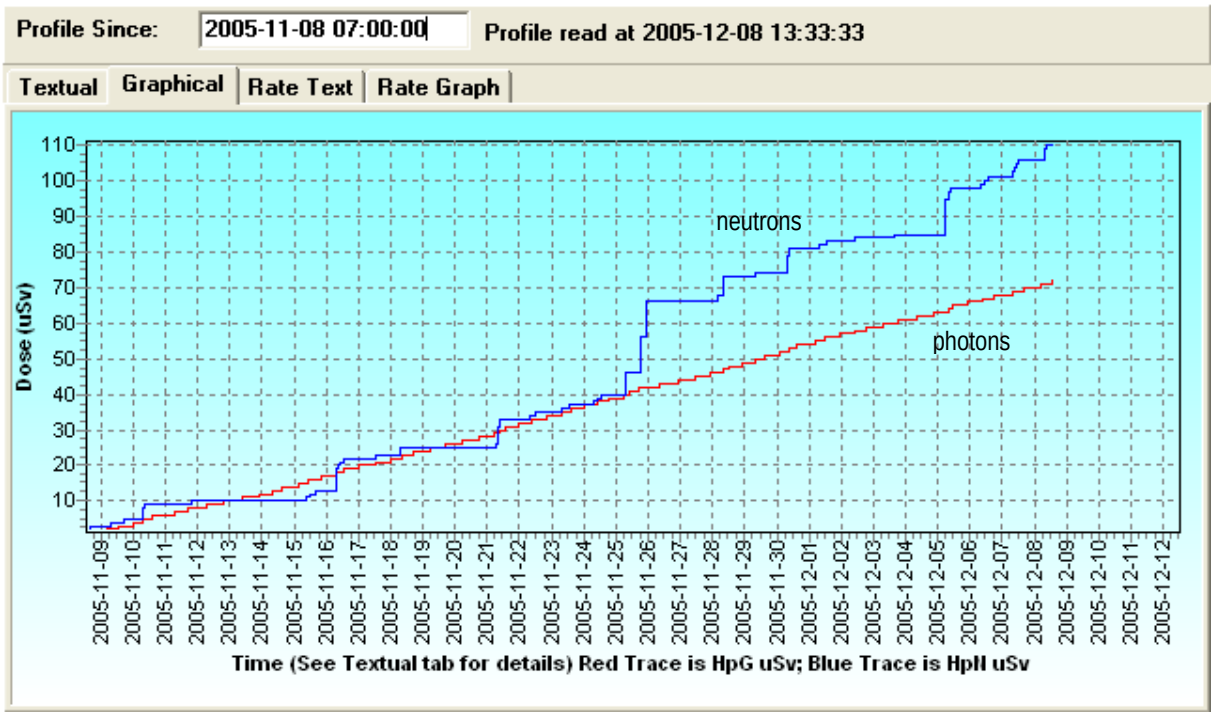

Figure 35. Graphical representation of the dose in L12 during one month (a total of 30 days including weekends).

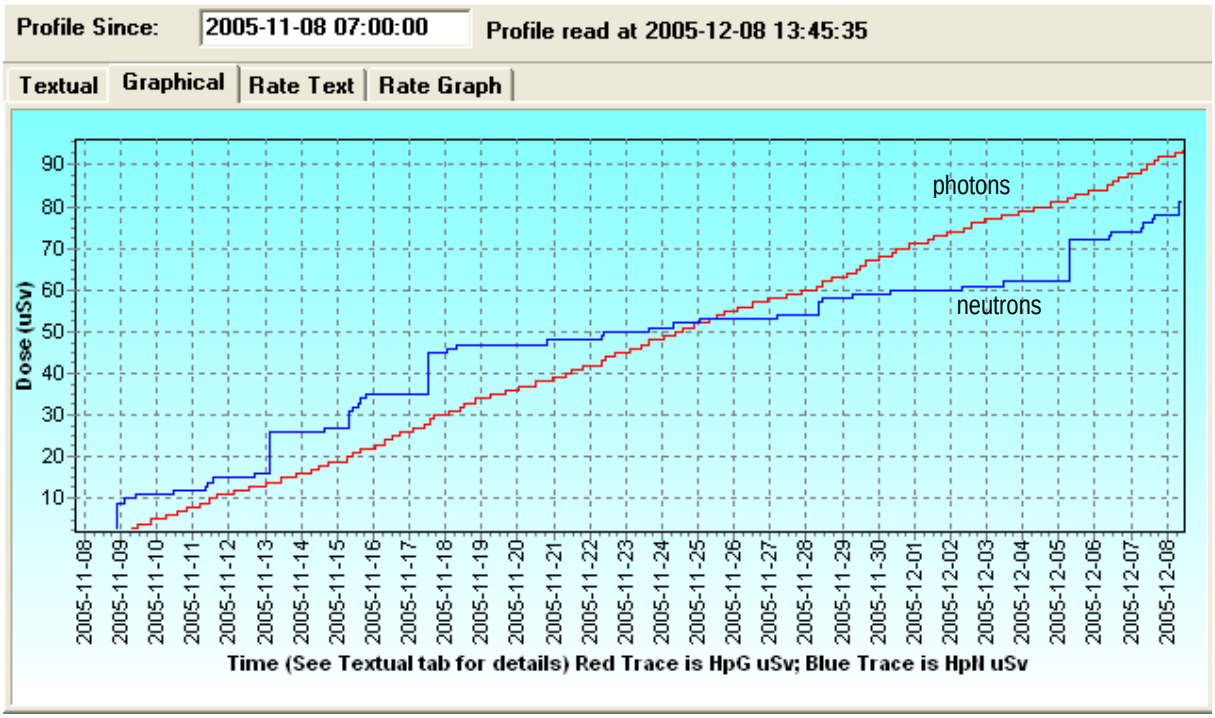

Figure 36. Graphical representation of the dose in L22 during one month (a total of 30 days including weekends).

The accumulated gamma and neutron dose, and the estimated total dose, during the personnel's time at work for one month (22 work days) in L12 and L22 respectively, is shown in table 13. The estimated doses per workday are presented in table 14.

Table 13. The accumulated gamma and neutron dose in the EPD-N2, and the estimated total dose in L12 and L22 respectively during 22 workdays.

Dose	L12 [µSv]	L22 [µSv]
Gamma	42	61
Neutron	76	42
Total	118	103

Table 14. The estimated gamma, neutron and total dose in L12 and L22 respectively per workday.

Dose	L12 [µSv]	L22 [µSv]
Gamma	1.9	2.8
Neutron	3.5	1.9
Total	5.4	4.7

As can be seen in the graphical representation of the dose (figure 35 and 36) the photon component increases continuously during the whole time while the neutron component changes significantly when the personnel are at work and when they leave work. The reason why the dosemeters showed high dose values late in the evening or during a weekend, when the personnel normally aren't at work, may be that the electronic personal dosemeters are sensitive to various electromagnetic fields. In L12 neutron dose is higher than the gamma dose by a factor of about 2. The neutron dose is higher in L12 than in L22 by a factor of about 2.

4.5 Results from all the monitoring devices

The estimated annual neutron dose equivalents from all the monitoring devices during patient treatments (and morning controls) are presented in table 15. The photon dose equivalent (γ) is also shown for the EPD-N2, the TLD and the FHT 752 BF_3 detector for comparison.

Table 15. The estimated annual (200 workdays) neutron dose equivalent (n) in L12 and L22 respectively. The photon dose equivalent (γ) is also shown for the EPD-N2, the TLD and the FHT 752 BF_3 detector for comparison.

	FHT 752 BF_3 *H*(10)* [*mSv/year*]	**BD-PND** *Hp(10)* [*mSv/year*]	**EPD-N2** *Hp(10)* [*mSv/year*]	**PADC** *Hp(10)* [*mSv/year*]	**TLD** *Hp(10)* [*mSv/year*]
L12	n=0.8 / γ=0.4	n=0.2	n=0.7 / γ=0.4	nd*	γ=0.7**
L22	n=0.2 / γ=0.2	n=0.02	n=0.4 / γ=0.6	nd*	γ=0.6**

*nd=not detectable
** Data taken from the monthly reported TLD values

The estimated dose equivalents in table 15 are not directly comparable since the monitoring devices have different properties, measure different operational quantity, and because of the different measuring points. However the results indicate that the neutron doses are higher for the personnel in L12. The neutron doses from personal dosemeters will depend on where the personnel are staying and for how long. The EPD-N2 dosemeters resulted in the highest neutron personal dose equivalent (0.7 mSv/year), being in the same order as the photon dose equivalent from the TLDs. However, this number may be overestimated since the EPD-N2 dosemeters may have been disturbed by various electromagnetic fields. The PADC dosemeters were sent to HPA in England for evaluation but they didn't report any dose, probably because the minimum reported dose for this dosemeter is higher than the other devices. The BF_3 FHT 752 presents the highest neutron dose equivalent, but this detector measures ambient dose equivalent, thus giving an overestimate of the effective dose.

Before assigning dose values from instruments measuring dose equivalent it is important to have knowledge of the behaviour of these devices and be aware of the uncertainties behind the measuring results. The first thing that needs to be considered is what quantity is measured, personal dose equivalent or ambient dose equivalent, since they have different relations to the effective dose. The personal dose equivalent is the operational quantity that a personal dosemeter should indicate, while the ambient dose equivalent is the quantity for area monitoring and used for hand-held instruments. The properties of the devices (sensitivity, cut-off energy, calibration source, directional dependence, operational quantity etc.) as well as how the devices are used and the measurement results interpreted, will influence the accuracy with which the operational quantities are to be determined.

5. Summary and Conclusions

This study shows that the neutron radiation levels were, in certain areas, higher than the photon component when using high-energy photon beams (18 MV). Furthermore, the neutron doses are higher to the personnel from L12 than L22 even though the numbers of 18 MV treatments are less in L12. This is probably mainly due to the poorer neutron shielding of the door in L12, since this door don't contain any paraffin.

The measurements with the area monitoring devices showed that the neutron equivalent dose rates when irradiating in L12 are highest outside the treatment door and inside the control room of L12, and at the hallway between the control rooms of L12 and L22. From these results and by the fact that the neutron angular distribution is nearly isotropic, figure 37 illustrates a thinkable way of the neutrons' scattering. The neutrons are mainly scattered through the door, not through the wall facing the control room.

The various types of neutron monitoring devices showed different numerical values due to their different characteristics. It is important to be aware of the uncertainties in neutron measurements and the influence of the energy distribution. Factors that will influence the choice of a monitoring method in neutron measurements include the operational quantity, environmental conditions, neutron field characteristics and the size and cost of the device. In this study the neutron spectrum is not known or determined which is necessary to have a better understanding of the instruments readings and in order to select the most appropriate detectors for a given situation.

The ambient dose equivalent takes all directions of radiation incidence into account with the same weight and therefore provides a reasonable overestimate of the effective dose in almost all irradiation geometries. A general relation between effective dose and personal dose equivalent is on the other hand difficult to give since the personal dose equivalent is dependent on whom and how the personal dosemeter is worn. The study at Ringhals nuclear power plant showed that the personal dose equivalent is a good estimate of the effective dose. According to ICRP 1996 the personal dose equivalent, under typical working conditions where neutron energies are distributed over a broad spectrum of energies, is a reasonable measure of the effective dose providing an overestimate of 25% or more. Taken this into account the personal dose equivalent is the most appropriate operational quantity for estimating the effective dose. The ambient dose equivalent is a rough approximation of the effective dose but is well suited for area monitoring.

To get an estimation of the effective dose, E, data from the known relationship between E and the ambient dose equivalent, H^*, in ICRU 57 have been used under the assumption that the neutron angular distribution is isotropic and that the dose on the floor and about one meter up is about the same. If using the H^* value from the BF_3 detector in L12, i.e. 0.8 mSv/year, the quotient E/H^* is expected to be less than 1, but probably more than 0.5 in the neutron energy range between 0.5 MeV and 10 MeV. Then the Hp value from the EPD-N2, i.e. 0.7 mSv/year, would be more reasonable than 0.2 mSv/year from the BD-PND detectors which are sensitive to higher energies but do not measure lower energies.

Additionally, the ^{3}He detector was half as sensitive as the BF_3 detector, i.e. giving about 0.4 mSv/year. With the E/H^* being between 0.5-1, this would result in an effective dose of around 0.2-0.4 mSv/year, thus being more close to the Hp value from the BD-PND in L12.

Eventually, the neutron effective dose to the personnel in L12 may be in the range between 0.2 mSv/year to 0.7 mSv/year.

Although the estimated effective doses are beneath the maximum permissible dose values (i.e. 50 mSv/year according to the Swedish Radiation Protection Authority) the neutrons can not be neglected and it is important to provide proper neutron shielding when using high-energy photon beams for the protection of the personnel. By having the ALARA-principle in mind, the measure that can be taken in order to reduce the neutron dose contribution to the personnel in L12 is to avoid 18 MV treatments in that bunker. If this is not practicable, one solution can be to build an additional “neutron stopping door” with hydrogen/boron-containing shielding material at the maze inside the treatment room that has to be closed during 18 MV treatments (see figure 38).

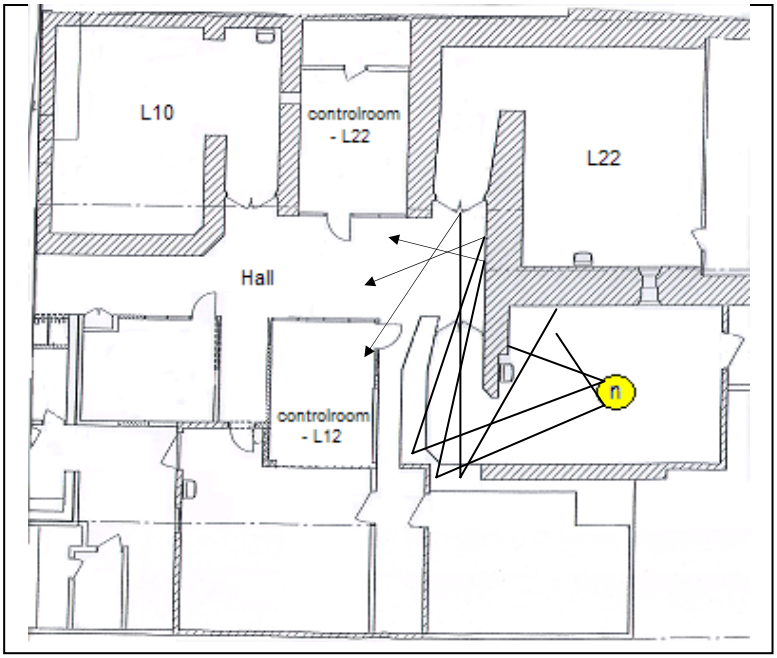

Figure 37. A sketch of how the neutrons are considered to be scattered from the treatment room in L12.

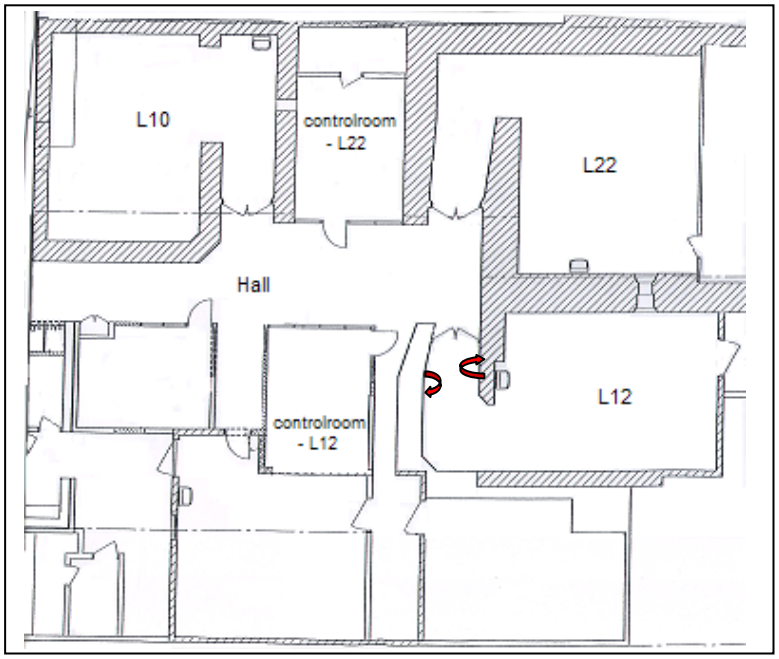

Figure 38. The solution with “neutron stopping door”.

6. Acknowledgements

First of all, I would like to thank my excellent supervisors Charlotte Thornberg and Sören Mattsson for all the engagement and support through this work, and for a great educational experience.

Thank you Anja Almén for coming to Malmö and letting me borrow your instrument.

Thank you Sven Bäck for your advices and concern, and thank you Peter Wallenius for helping me with the practical things.

Special thanks go to all the personnel at the departments of Radiation physics and oncology at UMAS who have helped me with my measurements.

7. Appendices

7.1 Appendix I

7.1.2 Definitions of quantities

Protection quantities

The **mean absorbed dose**, D_T, in a specified tissue or organ of the human body, T, is defined as:

$$D_T = (1/m_T)\int_{m_T} D\,dm \quad \text{or} \quad \varepsilon_T / m_T$$

where m_T is the mass of tissue or organ, D is the absorbed dose in the mass element dm, and ε_T is the total energy imparted in the tissue or organ.

The **equivalent dose**, H_T, in a tissue or organ, T, is defined as:

$$H_T = \sum_R w_R \cdot D_{T,R}$$

where $D_{T,R}$ is the average absorbed dose over the tissue or organ from radiation R, and w_R is the radiation weighting factor for radiation R, and the sum is performed through all kind of radiation that constitute the radiation field considered. The SI unit of the equivalent dose is (J kg^{-1}) and its special name is sievert (Sv). The values for radiation weighting factors as recommended by ICRP 1990 are given by table 16. For radiation types and energies that are not included in this table an approximation to w_R can be obtained by the calculation of the average quality factor, $\overline{Q}$, at a depth of 10 mm in the ICRU sphere (for the definition of the ICRU sphere see section 2.3.2 *Operational quantities*):

$$\overline{Q} = \frac{1}{D}\int_L Q(L)\cdot D(L)\cdot dL$$

where $D(L)dL$ is the absorbed dose at 10 mm between linear energy transfer values of L and $L + dL$, and $Q(L)$ is the corresponding quality factor.

Table 16. Values for radiation weighting factors [13].

Type of radiation	w_R
Photons, all energies	1
Electrons and muons, all energies	1
Neutrons,	
< 10 keV	5
10-100 keV	10
> 100 keV to 2 MeV	20
> 2-20 MeV	10
> 20 MeV	5
Protons other than recoil protons	
> 2 MeV	5
Alpha particles, fission fragments, heavy nuclei	20

The **effective dose** E is the sum of the equivalent doses in all tissues and organs, each multiplied by the appropriate tissue weighting factor, and is given by:

$$E = \sum_T w_T \cdot H_T$$

where H_T is the equivalent dose and w_T is the tissue weighting factor where the values are presented in table 17.

Table 17. Tissue weighting factors [13].

Tissue or organ	w_T
Gonads	0.20
Bone marrow (red)	0.12
Colon	0.12
Lung	0.12
Stomach	0.12
Bladder	0.05
Breast	0.05
Liver	0.05
Oesophagus	0.05
Thyroid	0.05
Skin	0.01
Bone surface	0.01
Remainder	0.05

Operational quantities

The **ambient dose equivalent**, *H*(d)*, at a point in a radiation field is the dose equivalent that would be produced by the corresponding expanded and aligned field in the ICRU sphere at a depth, *d*, on the radius opposing the direction of the aligned field. ICRU recommends that the depth 10 mm is used. The SI unit is (J kg^{-1}) and the special name is sievert (Sv).

The **personal dose equivalent**, $H_p(d)$, is the dose equivalent in soft tissue at an appropriate depth, d, below a specified point on the body. For strongly penetrating radiations (as for neutrons) the recommended depth is 10 mm. The SI unit is (J kg^{-1}) and the special name is sievert (Sv).

7.2 Appendix II

7.2.1 The software to FHT 752 BF_3 neutron probe

The FH 40 G-L10 unit can be connected to a PC via an infrared connection using a special software (FH40G.EXE). Only a few functions are available via the keys of the measuring unit, but can be exchanged to other functions via the software with *Functions - Configuration - Edit FH40G Menue Functions*. The functions available in the software are:

- Displaying the actual dose rate value that the unit is presently measuring in numerical or graphical form.
- Transferring measured data in a measurement file.
- Displaying and transferring measured data that is stored in the unit to the PC (history).
- Configuring the unit.

The measured values can be stored in a measurement file with *File - Open Logfile*. The measurement file is created and the measured data is stored in the scan interval you have defined. The logfile is closed with *File - Close Logfile* and viewed with *File - View Logfile*. New measured data can be appended to the existing data in the same file. Figure 39 shows the structure of the measurement file. The columns in the file contains date, time, dose rate value, a numerical value for "Dim" with the unit 0=µSv/h and a numerical value for "Status" with 01=external probe.

FH40G: Logfile: C:\DOCUME~1\ADMINI~1\SKRIVB~1\DRITA\L12MÄTNING
Ident .Text:: ESM Serial No.: 13448 242

Start yy.mm.dd	hh:mm:ss	Value	Dim	Status
05.11.30	07:19:45	0.1178E-2	0	01
05.11.30	07:19:50	0.1146E-2	0	01
05.11.30	07:19:58	0.1102E-2	0	01
05.11.30	07:20:03	0.1071E-2	0	01
05.11.30	07:20:07	0.1041E-2	0	01
05.11.30	07:20:12	0.1012E-2	0	01
05.11.30	07:20:18	0.9849E-3	0	01
05.11.30	07:20:23	0.9576E-3	0	01
05.11.30	07:20:28	0.9311E-3	0	01
05.11.30	07:20:33	0.9053E-3	0	01
05.11.30	07:20:38	0.8802E-3	0	01
05.11.30	07:20:43	0.8559E-3	0	01
05.11.30	07:20:48	0.8322E-3	0	01

Figure 39. The structure of the measurement file.

The measured values in the internal data memory of the unit can also be stored as history data either manually by using the function “STORE” on the instrument or automatically via the PC software such that it measures continuously. By this function the gamma dose rate can also be viewed but only a maximum of 256 measured values can be stored. The measured values can be transferred to the PC via the software with *Functions - History* and then *FH40G - History read*. Here you can activate automatic data storage.

Different kind of device settings can be changed with *Functions - Configuration*. If you click on the *Dose* button you can view the amount of the internal gamma dose, the external neutron dose and the total dose.

If there is no radiation source in the vicinity of the unit the instrument will display values corresponding to natural background. Since the number of impulses triggered by the background is very low and fluctuating you should repeat the reading after a few minutes and use the mean value of the measurements to obtain a reliable measured value. The measured pulse rate and the variation of the measured values are reduced as the dose rate increases.

The statistical variations are very high if the measuring time and the number of impulses is short and the count rates low. The measuring time and the number of impulses can be selected either manually or via the software with *Functions – Configuration* in the “Counter measurement” configuration area.

7.2.2 The software to EPD-N2 electronic personal dosemeter

A button on the front of the EPD-N2 allows the user to view some of the stored data and to perform certain functions. By turning the EPD-N2 off the dosemeter stops measuring radiation. The EasyEPD2 software can be used to read and write data to the EPD-N2 via an infrared communication link and display the data in a PC window. Once the software detects an EPD it automatically reads the data from the EPD and displays it in a window. The main window provides access to all EasyEPD2 operations via either the toolbar or the menu selections. In order to read the present values click on the *Read* button, and in order to write to the EPD click on the *Write* button.

The EPD stores changes in dose so that a profile of the dose over time can be recreated. The dose and the dose rate can be displayed either in textual or graphical form (see figure 35-36). The interval between stores can be set up on the *Set up Events* window. The profile can be read at any date and time by entering this in the *Profile Since* string, or just blank if you want all the dose profile. The *Save* button allows the dose profile to be saved to a file and the *Open* button allows a previously saved dose profile to be opened and viewed.

7.3 Appendix III

7.3.1 Tables

Table 18. L12 settings in numerical order during morning control.

	Energy	**Dose rate** [MU/min]	**Field size** [cm]	**Gantry angle**	**MU**
1.	6 MV	600	10*10	0º	200
2.	10 MV	600	10*10	0º	1000
3.	18 MV	600	10*10	0º	1000
4.	18 MV	600	10*10	0º	1000
5.	18 MV	600	10*10	0º	1000
6.	6 MeV	400	15*15	0º	200
7.	8 MeV	400	15*15	0º	200
8.	10 MeV	400	15*15	0º	200
9.	12 MeV	400	15*15	0º	200
10.	15 MeV	400	15*15	0º	200
11.	18 MeV	400	15*15	0º	200
12.	12 MeV	600	15*15	0º	150
13.	12 MeV	600	15*15	0º	150
14.	6 MV	600	10*10	0º	150
15.	6 MV	600	10*10	0º	150
16.	10 MV	600	10*10	0º	150
17.	10 MV	600	10*10	0º	150
18.	18 MV	600	10*10	0º	150
19.	18 MV	600	10*10	0º	150

Table 19. L12 settings during patient treatment. The indicated time is an approximate time when starting the patient treatment.

Time	**Energy** (MV)	**Gantry angle**	**Field size** [cm]	**MU** (open)	**MU** (wedge)	**MU** (total)
9.00	10	35	12*12	81	63	144
	10	195	12*13	77	60	137
	10	256	11*11	19	55	74
9.20	10	175º	11*14	-	57	57
9.40	18	240º	11*9	-	121	121
	18	219º	8*11	-	97	97
10.30	18	130º	10*7	-	124	124
	18	125º	9*15	-	83	83
10.50	18	-	16*18	21	138	159
13.00	18	232º	6*14	-	47	47
13.05	18	233	7*16	-	31	31
13.10	10	0º	10*10	88	55	143
	10	100º	8*10	19	61	80
	10	180º	9*9	101	-	101
14.00	10	270º	8*9	51	57	108
14.20	10	-	8*9	365	-	365

Table 20. L22 settings in numerical order during morning control.

	Energy	Dose rate [MU/min]	Fieldsize [cm]	Gantry angle	wedge	MU
1.	18 MV	500	10*10	0º	-	999
2.	6 MV	500	10*10	0º	-	999
3.	18 MV	600	15*30	0º	10º	100
4.	6 MV	600	15*30	0º	10º	100
5.	6 MV	500	10*10	0º	-	100
6.	6 MV	500	10*10	0º	-	100
7.	6 MV	500	10*10	0º	-	100
8.	18 MV	500	10*10	0º	-	100
9.	18 MV	500	10*10	0º	-	100
10.	18 MV	500	10*10	0º	-	100
11.	6 MeV	500	15*15	0º	-	100
12.	9 MeV	500	15*15	0º	-	100
13.	9 MeV	500	15*15	0º	-	100
14.	12 MeV	500	15*15	0º	-	100
15.	16 MeV	500	15*15	0º	-	100
16.	20 MeV	500	15*15	0º	-	100

Table 21. L22 settings in numerical order during patient treatment.

Patient	Energy (MV)	Gantry angle	Field size [cm]	MU (open)	MU (wedge)	MU (total)
8.00	18	0	9*10	69	-	69
	18	90	8*10	69	-	69
	18	180	9*10	35	-	35
	18	270	8*10	69	-	69
8.20	18	0	11*7	85	-	85
	18	90	9*7	-	91	91
	18	270	9*7	-	91	91
8.30	18	0	10*11	86	-	86
	18	90	8*11	-	89	89
	18	270	8*11	-	89	89
8.40	18	0	10*7	89	-	89
	18	90	10*7	-	95	95
	18	270	10*7	-	95	95
8.50	18	0	12*12	87	-	87
	18	90	11*12	-	95	95
	18	270	11*12	-	95	95
9.00	18	0	8*6	90	-	90
	18	90	8*6	-	99	99
	18	270	8*6	-	99	99
9.20	18	0	12*8	-	74	74
	18	90	12*8	72	-	72
	18	180	12*8	36	-	36
	18	270	12*8	72	-	72
9.40	18	0	13*11	-	76	76
	18	90	15*10	-	78	78
	18	180	13*11	31	-	31

	18	270	15*10	-	78	78
10.30	18	0	10*7	87	-	87
	18	90	10*7	-	93	93
	18	270	10*7	-	92	92
10.50	18	0	11*7	88	-	88
	18	90	10*7	-	94	94
	18	270	10*7	-	94	94
11.10	18	0	7*10	-	75	75
	18	90	8*7	74	-	74
	18	180	7*10	35	-	35
	18	270	9*7	74	-	74
11.20	18	0	9*10	71	-	71
	18	90	8*10	71	-	71
	18	180	9*10	36	-	36
	18	270	8*10	71	-	71
11.30	18	90	14*21	-	92	92
	18	270	14*21	-	103	103
11.50	18	90	13*13	-	109	109
	18	270	13*13	-	98	98
12.00	18	0	9*10	88	-	88
	18	90	9*10	-	93	93
	18	270	9*10	-	94	94
13.00	18	0	11*7	63	-	63
	18	90	10*8	60	-	60
	18	180	11*7	63	-	63
	18	270	10*8	60	-	60
13.20	18	90	13*18	-	90	90
	18	270	13*18	-	100	100
13.30	18	90	7*9	142	-	142
	18	270	7*9	142	-	142
14.00	18	0	9*9	91	-	91
	18	90	9*9	-	94	94
	18	270	9*9	-	94	94
14.20	18	127	14*10	-	60	60
	18	128	16*18	48	-	48
14.40	18	0	10*10	87	-	87
	18	90	10*10	-	92	92
	18	270	10*10	-	92	92
15.00	18	0	8*9	72	-	72
	18	90	8*9	72	-	72
	18	180	8*9	36	-	36
	18	270	8*9	72	-	72

8. References

1. National Council on Radiation Protection and Measurements (NCRP), Report No. 79, *Neutron Contamination from Medical Electron Accelerators*, USA 1984.
2. Almén A, Ahlgren L, Mattsson S, *Absorbed dose to technicians due to induced activity in linear accelerators for radiation therapy*, Phys. Med. Biol., 36 (6), 815-822, 1991.
3. Almén A, Ahlgren L, Mattsson S, *Leakage photon radiation around accelerators used for radiotherapy*, J. Radiol. Prot., 14 (4), 349-357, 1994.
4. Ongaro C, Zanini A, Nastasi U, Ródenas J, Ottaviano G and Manfredotti C, *Analysis of photoneutron spectra produced in medical accelerators*, Phys. Med. Biol. 45, L55-L61, 2000.
5. International Atomic Energy Agency (IAEA), Technical reports series No. 273, *Handbook on nuclear activation data*, Vienna, Austria 1987.
6. Mats Isaksson, *Grundläggande strålningsfyisk*, studentlitteratur Lund, 2002.
7. Anderson David W., *Absorption of Ionizing Radiation*, 1984.
8. R. Barquero, R. Mendez, H.R. Vega-Carrillo, M.P. Iniguez and T.M. Edwards, *Neutron spectra and dosimetric features around an 18 MV linac accelerator*, Health Phys, 88 (1), 2005.
9. Glenn F. Knoll, *Radiation Detection And Measurement*, 1979.
10. J R Greening, *Fundamentals of radiation dosimetry,* Medical physics handbooks 15, 2nd ed., 1985.
11. International Commission on Radiation Units and measurements (ICRU), *Conversion Coefficients for Use in Radiological Protection Against External Radiation*, Report No. 57, 1998.
12. International Commission on Radiological Protection (ICRP), *Conversion Coefficients for use in Radiological Protection against External Radiation*, Publication 74, Ann ICRP, 26 (3/4), 1996.
13. International Commission on Radiological Protection (ICRP), *1990 Recommendations of the International Commission on Radiological Protection*, Publication 60, Ann ICRP, 21(1-3), 1990.
14. International Commission on Radiation Units and measurements (ICRU), *Determination of Operational Dose equivalent Quantities for Neutrons*, Report No. 66, Journal of the ICRU, 1 (3), 2001.
15. Lennart Lindborg, SSI rapport 97:08, *Storheter för strålskyddsarbete*, 1997
16. Olsher, Richard H., Hsu, Hsiao-Hua, Beverding, Anthony, Kleck, Jeffrey H., Casson, William H., Vasilik, Dennis G., Devine, Robert T., *Wendi: An Improved Neutron Rem- meter*, Health Phys, 79 (2), 2000.
17. http://www.lanl.gov/orgs/n/n1/panda/00326408.pdf
18. http://www.bubbletech.ca/
19. http://www.hpa.org.uk/radiation/services/pms/datasheets/neutron.htm
20. http://www.thermo.com/eThermo/CMA/PDFs/Product/productPDF_24720.pdf
21. http://www.npl.co.uk/ionrad/training/nde/nde_2003_files/epd-n2_bill_croydon_summary.pdf
22. Björk A, *Personalstråldoser från neutroner vid strålbehandling*, 2002.